Identification of genetic interactions with *priB* links the PriA/PriB DNA replication restart pathway to double-strand DNA break repair in *Escherichia coli*

Aidan M. McKenzie,[1] Camille Henry (iD) ,[2] Kevin S. Myers,[3] Michael M. Place,[3] James L. Keck (iD) [1,*]

[1]Department of Biomolecular Chemistry, University of Wisconsin School of Medicine and Public Health, Madison, WI 53706, USA
[2]Department of Biochemistry, University of Wisconsin-Madison, Madison, WI 53706, USA
[3]Great Lakes Bioenergy Research Center, University of Wisconsin-Madison, Madison, WI 53726, USA

*Corresponding author: Department of Biomolecular Chemistry, University of Wisconsin School of Medicine and Public Health, 420 Henry Mall, Madison, WI 53706, USA. Email: jlkeck@wisc.edu

Abstract

Collisions between DNA replication complexes (replisomes) and impediments such as damaged DNA or proteins tightly bound to the chromosome lead to premature dissociation of replisomes at least once per cell cycle in *Escherichia coli*. Left unrepaired, these events produce incompletely replicated chromosomes that cannot be properly partitioned into daughter cells. DNA replication restart, the process that reloads replisomes at prematurely terminated sites, is therefore essential in *E. coli* and other bacteria. Three replication restart pathways have been identified in *E. coli*: PriA/PriB, PriA/PriC, and PriC/Rep. A limited number of genetic interactions between replication restart and other genome maintenance pathways have been defined, but a systematic study placing replication restart reactions in a broader cellular context has not been performed. We have utilized transposon-insertion sequencing to identify new genetic interactions between DNA replication restart pathways and other cellular systems. Known genetic interactors with the *priB* replication restart gene (uniquely involved in the PriA/PriB pathway) were confirmed and several novel *priB* interactions were discovered. Targeted genetic and imaging-based experiments with *priB* and its genetic partners revealed significant double-strand DNA break accumulation in strains with mutations in *dam*, *rep*, *rdgC*, *lexA*, or *polA*. Modulating the activity of the RecA recombinase partially suppressed the detrimental effects of *rdgC* or *lexA* mutations in Δ*priB* cells. Taken together, our results highlight roles for several genes in double-strand DNA break homeostasis and define a genetic network that facilitates DNA repair/processing upstream of PriA/PriB-mediated DNA replication restart in *E. coli*.

Keywords: DNA replication restart; *Tn*-seq; *priA*; *priB*; *priC*; *dnaT*; double-strand DNA breaks; MuGam-GFP

Introduction

Cell propagation relies on high-fidelity genome duplication. To accomplish this task, DNA replication complexes (replisomes) loaded onto origins of replication traverse the genome, utilizing parental DNA as templates as they synthesize new DNA strands. During this process, replisomes frequently collide with obstacles such as DNA damage or nucleo-protein complexes. In the most severe instances, these encounters cause replisomes to dissociate from the genome. In *Escherichia coli*, it is estimated that at least once per cell cycle a replisome prematurely dissociates from the chromosome (Cox *et al.* 2000; Mangiameli *et al.* 2017). Bacteria have therefore evolved mechanisms to reload replisomes at premature replication termination sites so that cells can complete genome duplication processes (Michel and Sandler 2017; Windgassen, Wessel, *et al.* 2018).

Genetic and biochemical studies have defined three pathways of DNA replication restart in *E. coli*: PriA/PriB, PriA/PriC, and PriC/ Rep (Fig. 1) (Lee and Kornberg 1991; Nurse *et al.* 1991; Masai *et al.* 1994; Sandler 2000; Sandler *et al.* 2001; McCool, Ford, *et al.* 2004; Heller and Marians 2005a; Manhart and McHenry 2013; Sandler

et al. 2021). Null mutations in *priA* or *dnaT* cause similar severe phenotypes, and both genes have been placed in the PriA/PriB and PriA/PriC pathways (Lee and Kornberg 1991; Nurse *et al.* 1991; Masai *et al.* 1994; McCool, Ford, *et al.* 2004). Conversely, minor phenotypes associated with mutations in *priC* or *rep* have placed them in the less frequently utilized PriC/Rep pathway, independent of PriA. *priB* or *priC* can each be deleted independently, but simultaneous deletion of both genes deactivates all three DNA replication restart pathways, resulting in lethality. In addition, a mutation encoding an ATPase- and helicase-deficient variant of PriA (*priA300*) elicits severe defects when paired with a *priB* deletion, but not a *priC* deletion (Sandler *et al.* 2001). Therefore, PriA helicase activity is likely required to facilitate the PriA/PriC pathway, but not the PriA/PriB pathway (Fig. 1). Each restart pathway recognizes abandoned DNA replication forks, remodels the forks to allow replisome loading, and reloads the replicative helicase (DnaB) with the help of its helicase loader (DnaC). After DnaB is reloaded, it recruits the remaining members of the replisome via protein–protein interactions (Tougu *et al.* 1994; Kim *et al.* 1996a,b; Costa *et al.* 2013).
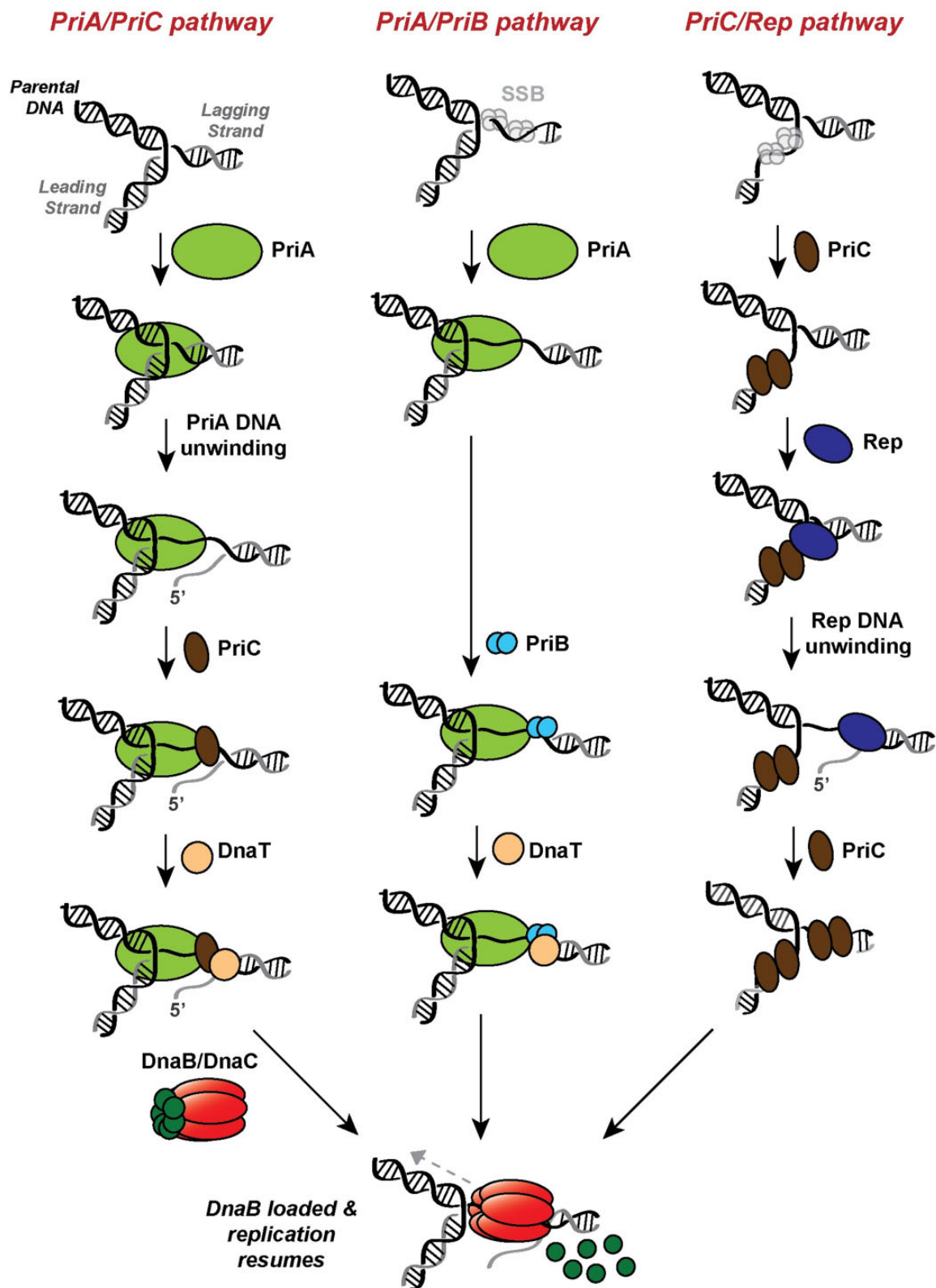
Fig. 1. Pathways of DNA replication restart in *E. coli*. PriA/PriC (left) and PriA/PriB (center) pathways efficiently recognize abandoned fork substrates with nascent leading strands, while the PriC/Rep (right) pathway prefers fork substrates with a leading strand gap. All 3 pathways recognize an abandoned fork, remodel the substrate (if needed) and recruit other replication restart proteins, and load the replicative helicase (DnaB) with the help of the helicase loader (DnaC) to restart DNA replication. The PriA/PriB pathway (center) is inactivated in Δ*priB* cells, the PriA/PriC (left) and PriC/Rep (right) pathways are inactivated in *priC::kan* cells, and the PriA/PriC (left) pathway is inactivated in *priA300* mutants.

Evidence suggests that different replication restart pathways can be preferentially utilized and/or that each operates on distinct substrates. For example, the PriA/PriB restart pathway appears to be favored following DNA recombination (Sandler *et al.* 1999). Mutations in *priB* are also more detrimental than *priC* when paired with a *holD* mutation, which increases instances of fork stalling and collapse (Flores *et al.* 2002). These results could indicate a heavier reliance on PriA/PriB than other pathways for replication restart. In addition, a *priB* deletion is synthetically lethal with mutations in *dam*, which encodes a DNA methyl transferase whose absence is linked to increased double-strand DNA breaks (DSBs) (Marinus 2000; Nowosielska and Marinus 2005; Boonsombat *et al.* 2006). This observation suggests that PriA/PriB replication restart could be important following DSB repair. Although *priC* disruption alone results in negligible phenotypic effects, in vitro evidence suggests that abandoned replication forks with long single-stranded (ss) DNA gaps between the nascent leading strand and parental duplex DNA may be recognized and remodeled efficiently by the PriC/Rep pathway, which could indicate its preference for specific abandoned DNA replication fork structures (Fig. 1) (Heller and Marians 2005a).

Candidate-based genetic studies have uncovered a limited number of genes linked to DNA replication restart, but a systematic study examining the potential importance of all genes as they relate to this process is lacking. Motivated by the idea that finding novel genetic interactions with each DNA replication restart pathway could help place each in a broader cellular context, we used transposon-insertion sequencing (Tn-seq; Langridge *et al.* 2009; van Opijnen *et al.* 2009; van Opijnen and Camilli 2013; Barquist *et al.* 2016) in Δ*priB*, *priC::kan*, and *priA300 E. coli* strains to identify genes that are conditionally important in each strain. Deletion of *priB* inactivates the PriA/PriB pathway, deletion of *priC* inactivates the PriA/PriC and PriC/Rep pathways, and the *priA300* allele disables the PriA/PriC pathway (Fig. 1) (Sandler 2000; Sandler *et al.* 2001; Windgassen, Wessel, *et al.* 2018; Sandler *et al.* 2021). The Δ*priB* Tn-seq screen yielded particularly informative results whereas the *priC::kan*, and *priA300* screens yielded far fewer hits, consistent with the PriA/PriB pathway serving as the primary replication restart mechanism in *E. coli*. The screen and additional genetic experiments corroborated prior genetic results in which *priC*, *rep*, and *dam* are conditionally essential or important in Δ*priB* cells. Strikingly, the screen also identified many new interactions between *priB* and genes involved in genome maintenance (*lexA*, *rdgC*, *uup*, *rdgB*, and *polA*) and other processes (*nagC*). Mutations in many of these genes produced strong growth defects in Δ*priB* cells, evidenced by plasmid retention, growth competition, and spot plating assays. Furthermore, *rep*, *lexA*, *polA*, and *dam* mutants were hypersensitive to ciprofloxacin, which induces DSBs. These mutant strains also accumulated DSBs in vivo and displayed significant cell filamentation, a common indicator of poor genomic maintenance. Lastly, some of the toxicity to Δ*priB* cells caused by mutations in *lexA* or *rdgC* appears to result from inappropriate and/or excessive RecA recombinase activity. These results highlight the importance of several genes in Δ*priB E. coli*, strengthen experimental evidence of the connection between the PriA/PriB restart pathway and DSB repair, and help elucidate the interplay between DNA repair and DNA replication restart processes.

Materials and methods
Strain construction
All strains used in this study are derivatives of *E. coli* MG1655 (Supplementary Table 1). To enhance the viability and ease of cloning, all strains (unless otherwise stated in Supplementary Table 1) carry the *sulB103* allele, encoding an FtsZ variant that resists SulA-mediated cell division inhibition (Bi and Lutkenhaus 1990; McCool, Long, *et al.* 2004). All plasmids and oligonucleotides used in this study are listed in Supplementary Table 2. To construct derivative *polA12(ts)* and MuGam-GFP strains, the method developed by Datsenko and Wanner (2000) was employed with some modifications, as described previously (Romero, Chen, *et al.* 2020). All strains constructed with P1 transduction utilized kanamycin selection, many of which relied on Keio collection strains as donors (Baba *et al.* 2006). Sources of strains and plasmids are provided in Supplementary Tables 1 and 2 (Singer *et al.* 1989; Cherepanov and Wackernagel 1995; Huang *et al.* 1997; Sandler *et al.* 1999; Datsenko and Wanner 2000; Bernhardt and de Boer 2004; Boonsombat *et al.* 2006; Shee *et al.* 2013; Byrne *et al.* 2014; Kim *et al.* 2015; Henrikus *et al.* 2019; Romero, Chen, *et al.* 2020). All chromosomal mutations were confirmed with PCR amplification flanking the locus of interest and, if necessary, verified with Sanger sequencing. We note that attempts to disrupt *priB* in two genome-wide gene replacement studies have suggested that *priB* may be essential in *E. coli* (Baba *et al.* 2006; Goodall *et al.* 2018). However, *priB* has been successfully deleted in *E. coli* when deletion is carried out in a manner that does not perturb expression of genes downstream of *priB* within its operon (Sandler *et al.* 1999; Sandler 2000). One of the two downstream genes encode an essential ribosomal protein gene (*rpsR*). The *priB* deletion allele that has been used successfully in prior experiments (del(*priB*)302) is used here (Supplementary Table 1).

Transposome preparation
Transposon mutagenesis was performed using the EZ-Tn5 <DHFR-1> transposon kit (Epicentre) and EK54/MA56/LP372 Tn5 transposase, a hyperactive variant (Goryshin and Reznikoff 1998). The Tn5 transposon was PCR amplified with oAM054 and Phusion polymerase (New England Biolabs). Tn5 transposase was purified as described previously (Bhasin *et al.* 1999; Byrne *et al.* 2014). Transposomes were prepared by incubating 2.5 pmol of Tn5 DNA with 0.5 nmol of Tn5 transposase in 20 µl for 3 h at room temperature before dialyzing into 1× TE for 3 h to remove salt prior to electroporation.

Generation of electrocompetent cells and in vivo transposition
E. coli strains were prepared for transposition as previously described (Byrne *et al.* 2014). Briefly, cells in mid-log phase were washed 3 times with ice-cold 10% v/v glycerol. In the final wash, cells were either resuspended in 10% v/v glycerol or glycerol-yeast extract medium (10% v/v glycerol, 0.125% w/v yeast extract, and 0.25% w/v tryptone), flash frozen with liquid nitrogen, and stored at −80°C. Dialyzed transposome (5 µl) was mixed with 100 µl of electrocompetent cells, electroporated, and immediately recovered in 1 ml of SOC medium (2% w/v tryptone, 0.5% w/v yeast extract, 0.05% w/v NaCl, 2.5 mM KCl, 10 mM MgCl₂, and 20 mM glucose) for 1 h. After recovery, dilutions of the cells were plated on Super Optimal Broth (SOB)-agar (2% w/v tryptone, 0.5% w/v yeast extract, 0.05% w/v NaCl, 2.5 mM KCl, 1.5% w/v agar, 10 mM MgCl₂, and 20 mM MgSO₄) containing 10 µg/ml trimethoprim to select for transposon-insertion mutants. Colony counts for each library were estimated by counting one-third of ∼10% of plates. To pool the mutants and construct libraries of ∼500,000 insertion mutants, 2 ml of Luria Broth (LB) (1% w/v tryptone, 0.5% w/v yeast extract, and 1% w/v NaCl) was added to each plate to scrape the colonies into a thick slurry. Care was taken to

sufficiently mix each slurry before archiving each in technical triplicate (in 50% glycerol) at −80°C.

Preparation of transposon-insertion DNA for sequencing

For sufficient sampling, 100 ml of LB (with 10 µg/ml trimethoprim) was inoculated to OD_{600} ~0.02 with each respective transposon-insertion mutant library and grown overnight at 37°C. Genomic DNA was purified using a Wizard Genomic DNA Purification Kit (Promega) and quantified using the QuantiFluor ONE dsDNA System (Promega). Genomic DNA was sheared to ~200-bp fragments with sonication. The resulting gDNA fragments were prepared for sequencing using NEBNext Ultra II DNA Library Prep Kit for Illumina (New England Biolabs). Bead-based size selection was used to enrich for 200-bp fragments prior to a 21-cycle splinkerette PCR utilizing a custom Tn5-enriching forward primer (oAM055) and custom indexed reverse primers for multiplexing (oAMrev) (Barquist et al. 2016). To ensure the quality and length of amplified DNA, a final bead-based size selection was employed. DNA was then sequenced with a NextSeq platform (Illumina) at the University of Michigan Advanced Genomics Core using a custom read primer (oAM058) to read the last 10 nt of the transposon before entering chromosomal DNA (to ensure reads corresponded to Tn5 insertions). To maintain sufficient sequence diversity on the flow-cell, a phiX174 DNA spike (20%) was also included in the run. A custom index read primer (oAM059) and standard Illumina primer (oAM112) were employed for sequencing the read indexes and PhiX174 DNA, respectively.

Tn-seq data analysis

Tn-seq sequencing files were trimmed with fastx_trimmer.pl version 0.0.13.2 (http://hannonlab.cshl.edu/fastx_toolkit) using default parameters except the first base to keep (-f flag) was set to 10 to remove transposon sequence. Individual samples were then split with fastx_barcode_splitter.pl, version 0.0.13.2 (http://hannonlab.cshl.edu/fastx_toolkit) using a file containing the sample ID and the individual barcode sequence used to split each sample into an individual FASTQ file. The barcode sequence was then removed from each read within each FASTQ file using Cutadapt, version 1.13 (Martin 2011). The trimmed FASTQ files were then aligned to the E. coli K-12 MG1655 genome (NC_000913.3) using Bowtie2, version 1.2 using default parameters (Langmead and Salzberg 2012). Conditionally important or essential genes were determined using TSAS, version 0.3.0 using Analysis_type2 for 2-sample analysis to compare transposon-insertion profiles of each mutant strain to the wt (Burger et al. 2017). Weighted read ratios were calculated as described previously (Burger et al. 2017). All other parameters were kept at the default settings. Tn-seq analysis is included Supplementary File 1.

Plasmid (priB-pRC7) retention assay

The priB-pRC7 plasmid is a lac⁺ mini-F (low-copy) derivative of pFZY1 (Bernhardt and de Boer 2004) containing the priB gene. PCR amplification of priB with oAM170 and oAM171 conferred ApaI restriction sites flanking the gene. The resulting PCR product and the empty pRC7 plasmid were digested with ApaI and ligated, yielding priB-pRC7. Gene deletions via P1 transduction were carried out after the cells had been transformed with the priB-pRC7 plasmid to help ensure the viability of each mutant tested. Once constructed, cultures were grown overnight in LB supplemented with 50 µg/ml ampicillin. The following day, cells were diluted 100× in LB and grown to ~0.2 OD_{600} shaking at 37°C. The cultures

were then placed at 4°C, serially diluted, and plated on SOB-agar containing X-gal (80 µg/ml) and IPTG (1 mM) to yield 50–500 colonies per plate. Most colonies were counted and imaged after 16 h incubations at 37°C, but plates used in Fig. 7 were incubated for 22 h to better visualize the small white colonies. Colony counts and analysis are included in Supplementary File 2.

Growth competitions

A growth competition experiment was used to determine if deleting rdgB conferred a measurable fitness defect in ΔpriB cells. Pairwise competitions were constructed where the fitness effect of a ΔrdgB mutation was examined in a priB⁺ or ΔpriB strain. To quantify the abundance of the ΔrdgB mutant, one strain within each competition was modified to carry a neutral ΔaraBAD mutation. When ara⁻ or ara⁺ strains are plated on medium containing tetrazolium and arabinose, they form red or white colonies, respectively. The individual strains of each competition were grown in isolation overnight at 37°C in LB, and then, equivalent volumes of each were mixed and diluted 100× in fresh LB. The cultures (now with competing strains) resumed growth at 37°C, and incubations were temporarily paused every 24 h to re-dilute (100×) in fresh LB and quantify the ΔrdgB mutant abundance by plating on LB agar (1% w/v tryptone, 0.5% w/v yeast extract, 1% w/v NaCl, and 0.75% w/v agar) with tetrazolium (0.005% w/v) and arabinose (1% w/v). The competitions were performed in biological triplicate and with pairwise alternation of the ΔaraBAD mutation (to ensure it did not produce a fitness effect). Colony counts and analysis are included in Supplementary File 2.

Spot plating experiments

Serial dilution spot plating was used to examine mutant sensitivities to ciprofloxacin and the effect of temperature and media on polA12(ts) strains. For ciprofloxacin sensitivity experiments, biological triplicate LB cultures were inoculated and grown overnight at 37°C, whereas strains used in the polA12(ts) experiment were grown at 30°C. The following day, the cultures were diluted to OD_{600} of 1.0 and 10× serial dilutions were prepared with LB or M9 (0.6% w/v Na_2HPO_4, 0.3% w/v KH_2PO_4, 0.05% w/v NaCl, 0.1% w/v NH_4Cl, 1 mM $MgSO_4$, 0.1 mM $CaCl_2$, and 0.1% w/v glucose) media. Serial dilutions (10 µl) ranging from 10^{-1} to 10^{-6} were spot plated and incubated at 37°C, unless stated otherwise. LB agar plates were incubated for 16 h, and M9 agar (0.6% w/v Na_2HPO_4, 0.3% w/v KH_2PO_4, 0.05% w/v NaCl, 0.1% w/v NH_4Cl, 1 mM $MgSO_4$, 0.1 mM $CaCl_2$, 0.1% w/v glucose, and 1.6% w/v agar) plates were incubated for 40 h before imaging.

Fluorescence and brightfield microscopy

An E. coli strain carrying MuGam-GFP (SMR14334; Shee et al. 2013) was derivatized to carry the sulB103 allele (wt) before P1 transduction deleted other genes of interest. Saturated cultures were diluted 100× and grown in LB for 30 min at 37°C to enter early exponential phase. MuGam-GFP expression was then induced at 100 ng/ml doxycycline and growth continued for an additional 2.5 h at 37°C. Cells were pelleted and resuspended in 1× PBS buffer (137 mM NaCl, 2.7 mM KCl, 10 mM Na_2HPO_4, and 1.8 mM KH_2PO_4) to OD_{600} of 1.0 and placed on ice. About 15 min prior to imaging, cell membrane stain FM 4-64 (5 mM) was added and 2–3 µl of cells were sandwiched between a 24 × 50 mM, no. 1.5 coverslip (Azer Scientific) and a 1.5% agarose pad. All cells were imaged at room temperature with a motorized inverted Nikon Ti-eclipse N-STORM microscope equipped with a 100× objective and ORCA Flash 4.0 digital CMOS C13440 (Hamatsu). Imaging was performed using NIS-Elements software with the microscope in epifluorescence mode. Cells were first

imaged in the brightfield (4.5 V, 100 ms exposure). Visualization of the cell membranes was performed in the DsRed channel to ensure the focusing (4.5 V, 50 ms exposure) and then MuGam-GFP was imaged in the GFP channel (4.5 V, 50 ms exposure). Growth, preparation, and imaging were performed for each strain in biological triplicate.

Analysis of cell features was performed with Fiji software (ImageJ) equipped with plugins as described previously: Single-Molecule Biophysics (https://github.com/SingleMolecule/smb-plugins) and MicrobeJ (Ducret *et al.* 2016). Briefly, the nd2 raw images for each strain (4–8 per replicate with a maximum difference of 2 images within triplicate) were concatenated together by channels. The image processing of each channel was carried out the same way and uniformly throughout the field of view. The scale of all images was corrected to fit the Hamamatsu camera scale. The brightfield and DsRed image stacks were auto-scaled while the GFP images were processed with discoidal averaging of 1–5 and intensity scale set at 0–300. Both brightfield and DsRed channels were cleaned by running a Bandpass filter 10_2 with auto-scale 5, a rolling sliding stack of 10, and an enhance contrast of 0.1. Channel stacks were converted to 8 bits before analysis in MicrobeJ. For the analysis, hyperstacks combining only the FM 4-64 and GFP channels were generated in MicrobeJ. From these hyperstacks, cell outlines were detected in the DsRed channel using the default method with a threshold of +25. Within identified cells, GFP foci were detected using the maxima features as foci with a Gaussian fit constraint. The exact setup used to identify bacteria and MuGam-GFP foci in MicrobeJ is available (Final Bacteria setup 1_5 foci 90) as a .xml file. After automatic detection, cells were manually sorted to remove poorly fitting outlines or outlines fitting to cells out of focus. Cell features analysis acquired with MicrobeJ (cell ID, cell length, number of foci per cell, foci intensity, and size) was exported as .csv files. Plots and statistical analysis were generated and performed with GraphPad Prism software. At least 650 single cells were analyzed for each condition. Fluorescence and brightfield microscopy data/analysis is included in Supplementary File 3.

Results

Tn-seq identifies genetic interactions in Δ*priB*, *priC::kan*, and *priA300* strains

DNA replication restart functionally integrates with other processes in *E. coli*. However, experiments to probe this integration have been limited to candidate genetic and biochemical studies. To systematically map connections between DNA replication restart and other processes, we performed *Tn*-seq screens to assess the tolerance of gene disruption in mutant strains restricted to specific pathways of DNA replication restart. Deleting *priB* inactivates the PriA/PriB pathway, the *priA300* allele (which produces an ATPase- and helicase-deficient PriA variant) disables the PriA/PriC pathway, and a *priC*-null mutation (*priC::kan*) inactivates the PriA/PriC and PriC/Rep pathways (Fig. 1) (Sandler 2000; Sandler *et al.* 2001; Windgassen, Wessel, *et al.* 2018; Sandler *et al.* 2021). We therefore carried out screens in each of these backgrounds to independently identify genes with enhanced importance in each genetic background.

Isogenic wild-type (*wt*), Δ*priB*, *priA300*, or *priC::kan E. coli* strains were constructed with the *sulB103* mutation, which encodes an FtsZ variant resistant to SulA-mediated cell division inhibition and bolsters the viability of DNA replication restart mutants (Bi and Lutkenhaus 1990; McCool, Long, *et al.* 2004). Three biological replicate Tn5 transposon libraries with ~165,000 transposon-insertion mutants were generated for each strain to yield ~500,000 total insertion mutants in each genetic background. Viable transposon-insertion mutants were selected by plating on SOB solid medium supplemented with trimethoprim (ensuring Tn5 insertion). After pooling to assemble each individual replicate, the libraries were subjected to overnight growth in LB liquid medium forcing direct competition among transposon-insertion mutants. Successive replication initiation events launch prior to cell division in cells grown in rich media, resulting in more than two replication forks on each chromosome (Withers and Bernander 1998; Fossum *et al.* 2007; Hill *et al.* 2012). As a result, the *Tn*-seq screen selected for mutants that allow growth under normal DNA repair and replication restart levels in each of the test strains. Following growth in LB, genomic DNA was isolated from each replicate and prepared for next-generation sequencing. The resulting sequencing data revealed the location of transposon insertions as well as relative transposon-insertion mutant abundance. Each gene in our analysis was assigned a normalized weighted read ratio based on insertion tolerance in the mutant strain compared to the *wt* strain (Burger *et al.* 2017). Positive or negative weighted read ratios reflect gene disruptions that were tolerated better or worse, respectively, in the *wt* strain compared to the mutant strain. Genes with few or no insertions were considered important for growth, and such profiles within the *wt* control strain implicated genes as being essential under the tested growth conditions. By comparing insertion profiles of the *wt* and mutant strains, several genes that were conditionally important in replication restart mutant strains were identified.

Tn-seq data identified several genes as conditionally important in *E. coli* cells lacking the PriA/PriB restart pathway (Δ*priB*). Genes with the strongest *priB* genetic interactions evidenced by weighted read ratios (Fig. 2) and unique insertions (Supplementary Fig. 1a) were selected for subsequent study, except for *rplI* because of its inclusion in the same operon as *priB*. Corroborating previous studies, the screen implicated *rep* (log_{10} weighted read ratio = 4.11) and *dam* (2.35) as genetic interactors with *priB* (Sandler 2000; Boonsombat *et al.* 2006). *priC* (1.25) was a less prominent hit than would be expected given its known synthetic relationship with *priB* (Sandler 2000). However, the modest weighted read ratio for *priC* was due to the limited number of transposon insertion in the *wt* control strain—the *priC* gene tolerated no transposon insertions in the Δ*priB* strain. The expected lethality of a Δ*priB* Δ*priC* double deletion strain was later confirmed. In addition to known genetic interactions, bioinformatic analysis and manual curation of the *Tn*-seq data implicated a variety of novel genes as genetic interactors with *priB*: *rdgC* (4.06), *nagC* (3.29), *uup* (3.98), *rdgB* (1.86), *polA* (2.80), and *lexA* (2.58) (Fig. 2). These top hits (apart from *nagC*) have noted roles in genome maintenance but have not been genetically linked to *priB* prior to this study (d'Ari 1985; Savic *et al.* 1990; Plumbridge 2001; Bradshaw and Kuzminov 2003; Drees *et al.* 2006; Murat *et al.* 2006; Pennetier *et al.* 2008; Romero, Armstrong, *et al.* 2020). The abundance of conditionally important genes in Δ*priB* cells is consistent with PriA/PriB serving as the primary DNA replication restart pathway in *E. coli* (Flores *et al.* 2002).

Disparities in the transposon-insertion profiles between the *wt* control and *priC::kan* or *priA300* mutant strains were relatively modest, resulting in smaller overall weighted read ratios for genes (Supplementary Fig. 1, b and c). This likely was due to basal stress levels being tolerated in both mutant strains since each retained the PriA/PriB pathway (Sandler 2000; Sandler *et al.* 2001, 2021; Windgassen, Wessel, *et al.* 2018). One exception was the clear underrepresentation of transposon insertions in *rep* (4.11) within the *priA300* strain (Supplementary Fig. 1c). This result is
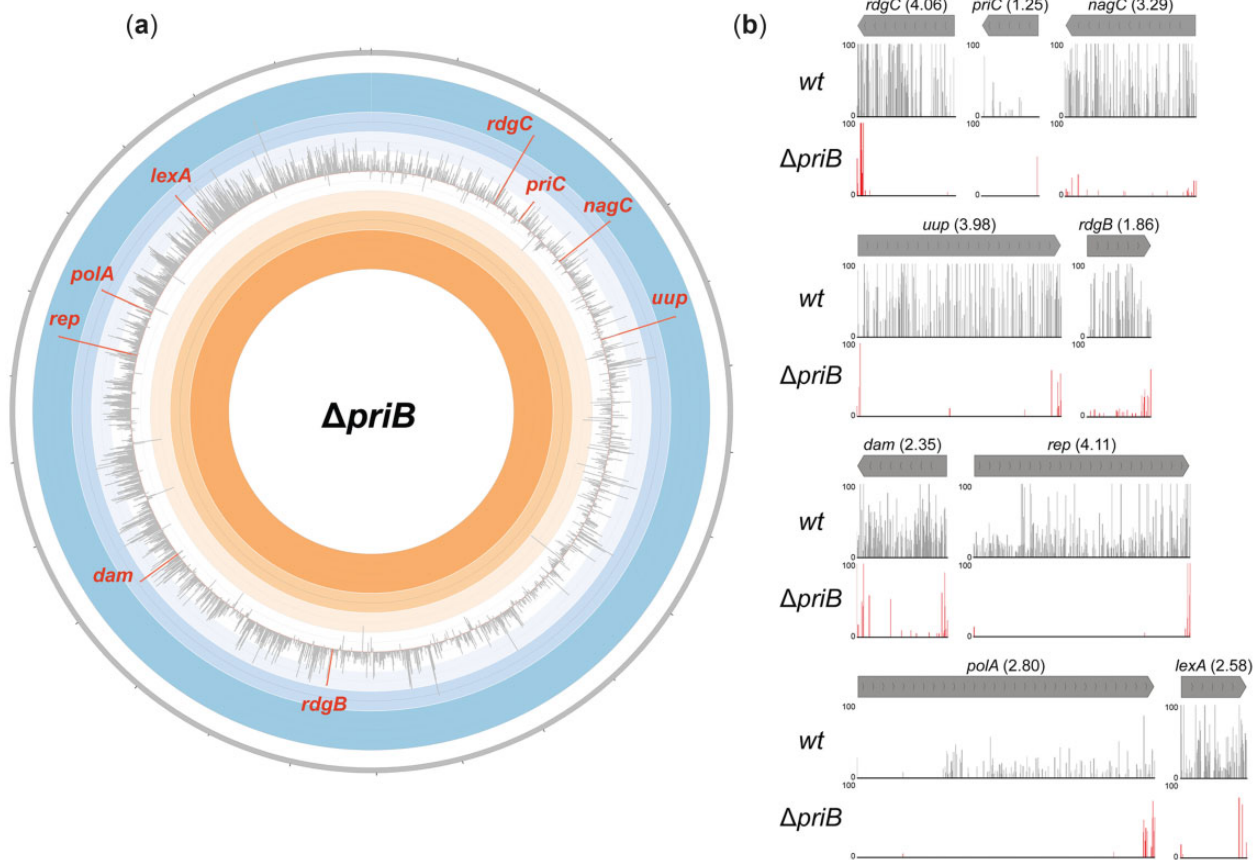
Fig. 2. Tn-seq results in ΔpriB E. coli. a) Circos plot depicting the results of the Tn-seq screen in ΔpriB cells. The effect of single-gene disruption via transposon-insertion was determined by comparing Tn-seq read profiles in wt vs ΔpriB conditions, yielding a weighted read ratio. Each bar in the Circos plot represents the weighted read ratio ($\log_{10}$) of a single gene where extension into the blue or orange region corresponds to a detrimental or beneficial, respectively, effect of gene disruption. Genes with fewer than three unique transposon-insertions per replicate in the wt condition are omitted. The individual disruption of many genes involved in genome maintenance produced some of the most prominent defects and were the focus of the study. Bars for notable genes (rdgC, priC, nagC, uup, rdgB, dam, rep, polA, and lexA) are highlighted. b) MochiView plots for genes highlighted in (a) comparing transposon-insertion locations and read abundance. The corresponding weighted read ratio for each gene is included in parentheses. The maximum read height displayed is 100.

consistent with the previously described conditional importance of rep in priA300 cells (Sandler 2000; Mahdi et al. 2006; Michel and Sandler 2017). No other genes were identified with significantly different insertion profiles with respect to weighted read ratios in either the priC::kan or priA300 strains relative to the wt control (Supplementary Fig. 1, b and c). Interestingly, priB had a lower than anticipated weighted read ratio in the priC::kan screen, but this was due to a very small number of transposon insertions within priB for all strains. This is consistent with a prior observation that the E. coli priB gene receives fewer insertions in transposition screens than would be predicted for a gene of its size, which may be due to polar effects on the essential rpsR gene and/ or rplI directly downstream of priB within the same operon (Goodall et al. 2018).

Mutations in priC, rep, lexA, dam, rdgC, uup, nagC, or rdgB confer a dependence on priB

Given the importance of the PriA/PriB pathway as reflected by the ΔpriB Tn-seq screen results, the remainder of our study interrogated the relationship between priB and its genetic interactors. A plasmid retention assay was first used to measure the impact of mutations in genes identified in our Tn-seq screen on cell viability with or without chromosomal priB (Bernhardt and de Boer 2004;

Romero, Chen, et al. 2020). The assay followed retention of an unstable, low-copy plasmid (priB-pRC7, which contained priB and the lac operon) in priB$^+$ or ΔpriB strains with chromosomal deletions of the lac operon and genes identified as conditionally important in the ΔpriB Tn-seq screen. Plasmid retention or loss was marked by colony color (blue or white, respectively) when plated on SOB-agar containing X-gal and IPTG (Fig. 3). Importantly, these priB-pRC7 retention experiments did not rely on constructing double mutant strains, which are particularly susceptible to suppressor mutations during liquid growth experiments (Sandler 2000). Instead, the strains were tested in a restricted experimental window following priB-pRC7 plasmid loss (immediately prior to plating).

In line with previous genetic results, deletion of priC or rep in ΔpriB cells resulted in persistent retention of priB-pRC7, strongly supporting their known synthetic lethal relationships with priB (Fig. 3, c and d) (Sandler 2000). Screening of a newly identified genetic interaction revealed that lexA and priB also form a synthetic lethal pair in our genetic background (Fig. 3e). LexA is a transcriptional repressor that undergoes auto-proteolysis to induce the SOS DNA-damage response genes (d'Ari 1985; Giese et al. 2008). As a result, disruption of lexA causes constitutive SOS expression, and it follows that induction of one or more SOS genes is toxic to
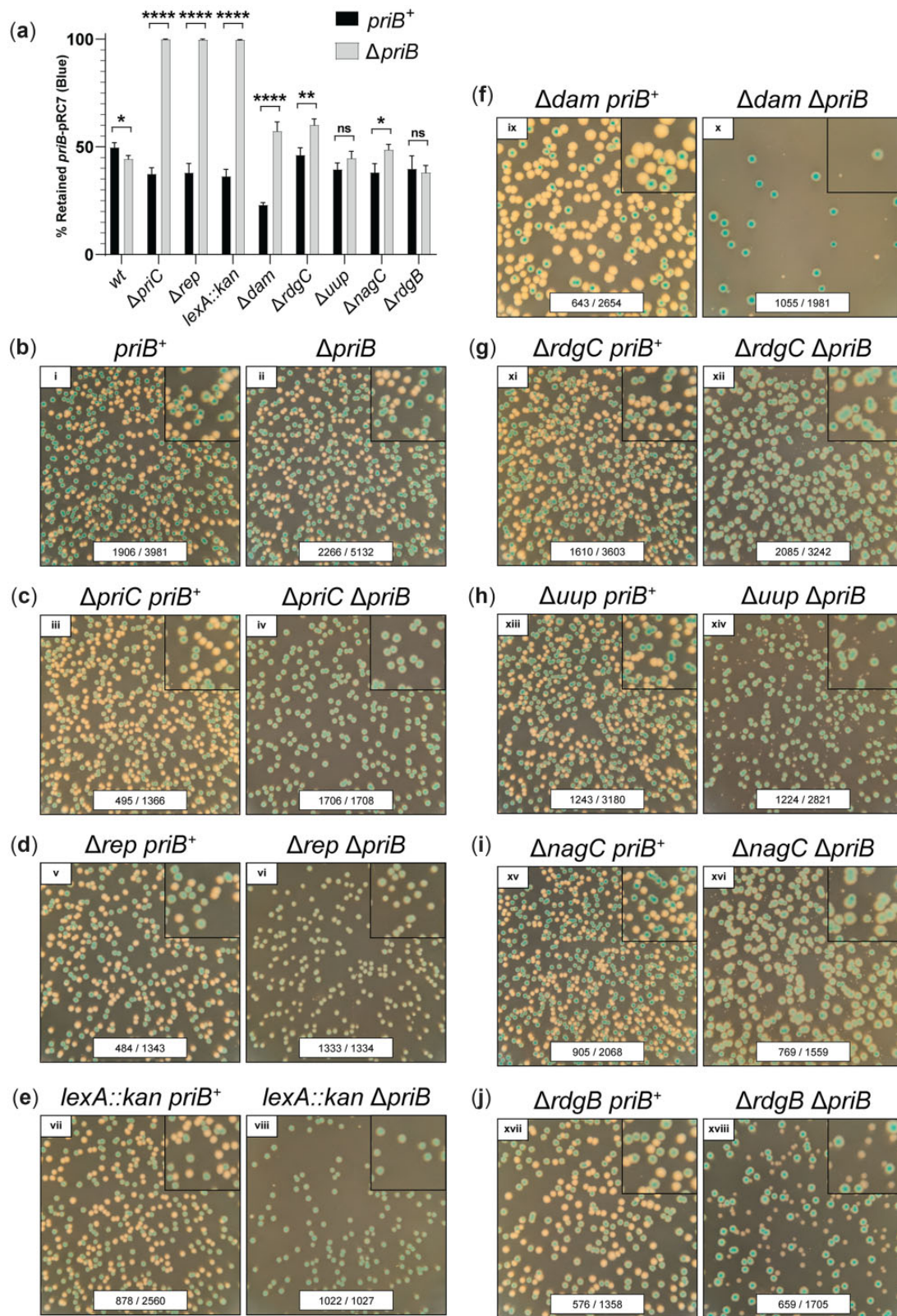
Fig. 3. Importance of specific genes in Δ*priB E. coli*. Genes implicated as conditionally important or essential in the Δ*priB* Tn-seq screen were tested with a plasmid retention assay. a) Percentages of colonies that retained *priB*-pRC7 plasmid are shown. Mean values are depicted with error bars representing standard error of the mean. Statistical significance (unpaired student *t*-test) for each strain pair is displayed: $P < 0.05$ (*), $P < 0.01$ (**), and $P < 0.0001$ (****). Representative images from *priB*-pRC7 assay plates are shown as follows: (b) *wt*, (c) Δ*priC*, (d) Δ*rep*, (e) *lexA::kan*, (f) Δ*dam*, (g) Δ*rdgC*, (h) Δ*uup*, (i) Δ*nagC*, and (j) Δ*rdgB*. Each plate image includes raw colony counts for each condition (# of blue colonies/# of total colonies). To better visualize small white colonies, 2.25× magnified insets are included in the upper right-hand corner for each plate image. Each plate was incubated at 37°C for 16 h.

ΔpriB cells (McCool, Long, *et al.* 2004). For mutations in *priC*, *rep*, or *lexA*, the extent of plasmid loss was equivalent to control levels in *priB*⁺ cells (Fig. 3, a–e).

In contrast to the robust and consistent *priB*-pRC7 retention characteristics of the mutant strains described above, mutations in *dam*, *rdgC*, *uup*, *nagC*, or *rdgB* did not entirely prevent plasmid loss when paired with a *priB* deletion (Fig. 3, f–j). However, compared to plasmid-containing blue colonies, white colonies (lacking *priB*-pRC7) formed by these double mutants were smaller, indicative of reduced growth rates. For Δ*rdgB* Δ*priB*, the disparity in size between blue and white colonies was modest (Fig. 3J). However, when other gene deletions (Δ*dam*, Δ*rdgC*, Δ*uup*, or Δ*nagC*) were paired with Δ*priB*, the resulting plasmid-less white colonies were particularly small and difficult to quantify (Fig. 3, f–i). As a result, disparities in colony size for many of these strains is likely a better proxy of cellular health than a plasmid retention percentage (Fig. 3a).

Previous studies have noted a synthetic lethal relationship between *dam* and *priB*, suggesting that DSBs accumulating in Δ*dam* cells are preferentially funneled into the PriA/PriB pathway for restart following repair (Boonsombat *et al.* 2006). While our data do not confirm a synthetic lethal relationship between *dam* and *priB*, our *priB*-pRC7 retention results identify a strong conditional importance of *dam* in Δ*priB* cells based on a disparity in colony size (Fig. 3f). The decreased growth rate of white colonies evident in the assay also confirmed the conditional importance of *rdgC*, *uup*, *nagC*, and *rdgB* in Δ*priB* cells (Fig. 3, g–j). While RdgC (an inhibitor of RecA recombinase activity), Uup (a branched DNA intermediate binding protein), and RdgB (a noncanonical purine pyrophosphatase) have been implicated in genome maintenance processes, these results now map the genes' interactions with the PriA/PriB restart pathway (Bradshaw and Kuzminov 2003; Moore *et al.* 2003; Drees *et al.* 2006; Murat *et al.* 2006; Romero, Armstrong, *et al.* 2020; Romero, Chen, *et al.* 2020). Surprisingly, conditional importance in Δ*priB* cells extended to *nagC*, which encodes a transcriptional repressor that coordinates *N*-acetylglucosamine biosynthesis but has no known role in DNA metabolism (Plumbridge 2001; Pennetier *et al.* 2008). These data support the notion of conditional importance for *dam*, *rdgC*, *uup*, *nagC*, or *rdgB* in Δ*priB* cells (Fig. 3, f–j).

Disruption of *rdgB* in a Δ*priB* strain confers a fitness defect

The disparity of colony sizes in the *priB*-pRC7 retention assay provided only moderate evidence that *rdgB* is conditionally important in Δ*priB* cells. To examine the *rdgB priB* genetic relationship more confidently, the fitness of strains combining *rdgB* and *priB* mutations was tested in a growth competition assay. In this assay, the effect of a *rdgB* deletion was examined within a *priB*⁺ competition (*priB*⁺ vs Δ*rdgB priB*⁺) and within a Δ*priB* competition (Δ*priB* vs Δ*rdgB* Δ*priB*). A synthetic fitness defect would result in selective loss of Δ*rdgB* Δ*priB* in the latter competition. A reporter mutation (Δ*araBAD*) in one strain of each competition was utilized to quantify the relative Δ*rdgB* abundance throughout each competition. As expected for a synthetic *rdgB priB* relationship, simultaneous deletion of both genes caused a pronounced fitness defect within 24 hours when grown in competition with *rdgB*⁺ Δ*priB* cells (Fig. 4a, red). In contrast, Δ*rdgB priB*⁺ cells exhibited no detectable fitness defect when grown in competition with *wt* cells, as evidenced by steady relative abundance within the *priB*⁺ competition (Fig. 4a, black). These results confirm that *rdgB* is not essential in a Δ*priB* strain, but that it is conditionally important. The mild defect in growth rate of Δ*rdgB* Δ*priB* colonies (Fig. 3j) but clear fitness defect (Fig. 4a) align well with *rdgB* as a relatively weak hit from our Δ*priB* *Tn*-seq screen (Fig. 2 and Supplementary Fig. 1a).

Polymerase I activity is conditionally important for Δ*priB* cells

The *Tn*-seq screen suggested a genetic relationship between *priB* and *polA* (Fig. 2). However, the essential nature of *polA* ruled out simple gene deletion experiments to further examine this link (Joyce and Grindley 1984; Joyce *et al.* 1985). Inspection of the transposon-insertion profiles (Fig. 2b) suggests that only certain regions of *polA* are conditionally important for survival in Δ*priB* cells. Specifically, regions of the gene that encode the C-terminal
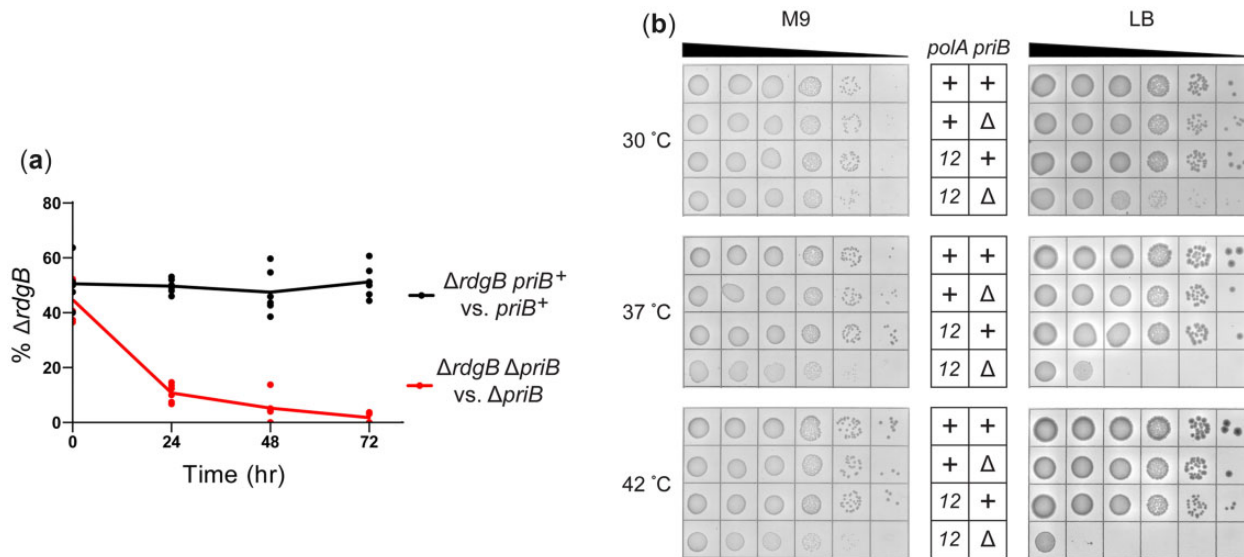
Fig. 4. Importance of *rdgB* and Pol I polymerase activity in Δ*priB* E. coli. a) Growth competition examining the effect of a *rdgB* mutation on fitness for *priB*⁺ or Δ*priB* strains. Trendlines for each series intersect the mean, and biological triplicate data points are presented for competitions done in duplicate. b) Effect of the *polA12(ts)* allele on *priB*⁺ or Δ*priB* strains. Strains were spot plated on minimal (M9, left) or rich (LB, right) media and incubated at 30, 37, or 42°C. Dilutions (from left to right) are 10× serial dilutions from normalized overnight cultures.

3′-5′ exonuclease and polymerase domains of DNA polymerase I (Pol I) poorly tolerated transposon insertions in the Δ*priB* strain compared to the *wt* strain. These two domains comprise the Klenow fragment of Pol I (Klenow and Henningsen 1970). Conversely, the portion of *polA* encoding the 5′–3′ exonuclease domain poorly tolerated insertions in both the Δ*priB* and *wt* strains, consistent with this domain encoding the essential function of *polA* in rich media (Joyce and Grindley 1984).

To test the importance of the polymerase activity of Pol I in Δ*priB* cells, we utilized the *polA12(ts)* mutant allele. This mutation encodes a Pol I variant with severely inhibited polymerase activity at high temperatures (Lehman and Chien 1973; Uyemura and Lehman 1976; Camps and Loeb 2005). In addition, *polA12(ts)* is synthetically lethal with a *priA* mutation under nonpermissive conditions (Lee and Kornberg 1991; Kogoma 1997). Spot plate assays examined the viability of *polA12(ts)* Δ*priB* and control strains at increasing temperatures on LB (rich) or M9 (minimal) media to determine the conditional importance of Pol I polymerase activity (Fig. 4b). In agreement with the *Tn*-seq screen results, *polA12(ts)* Δ*priB* cells displayed temperature-sensitive synthetic defects on LB media. At 37°C, the double mutant was at least 100x less viable than the *polA12(ts)* *priB*⁺ strain, and this effect was exacerbated to ∼1,000x at 42°C. The *polA12(ts)* mutation appeared to cause a reduced growth rate of Δ*priB* cells even at 30°C, evidenced by the smaller colony sizes in the double mutant. Based on previous studies, this detrimental effect is likely driven by reduced polymerase activity (Lehman and Chien 1973; Uyemura and Lehman 1976; Camps and Loeb 2005). Interestingly, *polA12(ts)* Δ*priB* strain viability was significantly restored by plating on M9 (minimal) media. This partial suppression likely stems from fewer concurrent rounds of DNA replication initiation in minimal media, and it underpins the importance of efficient genome maintenance in nutrient-rich environments (Withers and Bernander 1998; Fossum *et al.* 2007; Hill *et al.* 2012).

Mutations in *rep*, *lexA*, *polA*, or *dam* cause sensitivity to exogenous DSBs

A prior study demonstrated a synthetic lethal relationship between *priB* and *dam* and suggested that this relationship may result from DSBs formed in *dam* mutants being funneled into the PriA/PriB restart pathway following their repair (Boonsombat *et al.* 2006). Therefore, we examined whether other genes identified in the Δ*priB* *Tn*-seq screen could be driving toxicity through enhanced DNA-damage accumulation. Mutant strains were spot plated onto LB supplemented with sublethal concentrations of the DSB-inducing antibiotic ciprofloxacin (Fig. 5) (Willmott and Maxwell 1993; Tamayo *et al.* 2009). A *recA* deletion strain was utilized as a positive

control for hypersensitivity (Klitgaard *et al.* 2018) and was inviable at 5 ng/ml ciprofloxacin. Notably, a Δ*priB* strain also exhibited extreme hypersensitivity and was inviable at 10 ng/ml ciprofloxacin. Similar sensitivity was reported recently for Δ*priB* *E. coli* (Mallikarjun and Gowrishankar 2022). Mutations in *rep* and *lexA* led to viability defects at 10 ng/ml ciprofloxacin but were significantly more resistant than Δ*priB* or Δ*recA* strains. At 15 ng/ml ciprofloxacin, the Δ*dam* and *polA12(ts)* mutants began to display defects as well. We note that the reduced growth rate of *dam* mutants in the presence of DNA-damaging agents has been linked to a reduction in replication initiation, which may be leading to smaller colony sizes with inhibitory ciprofloxacin concentrations (Sutera and Lovett 2006). Other mutants identified in the Δ*priB* Tn-seq screen were not sensitized to ciprofloxacin (Supplementary Fig. 2). These results suggest cellular roles for *priB*, *recA*, *dam*, *rep*, *lexA*, and *polA* in prevention and/or repair of DNA damage in vivo.

Visualizing DSBs in vivo with MuGam-GFP

Sensitization of *rep*, *lexA*, *polA*, and *dam* mutants to ciprofloxacin suggests that these mutant strains may also have enhanced levels of endogenous DSBs. To test this hypothesis, mutations were transduced into an *E. coli* strain (SMR14334) encoding inducible MuGam-GFP, a DSB sensor protein, and the extent of DSB accumulation was determined in vivo with fluorescence microscopy (Supplementary Fig. 3, a, b, and d) (Shee *et al.* 2013).

MuGam-GFP foci were more abundant in a *dam* deletion strain than in the *wt* strain (Fig. 6, a and b) (Nowosielska and Marinus 2005). These mutant cells were also severely filamented which is a hallmark of DNA damage in *E. coli* (Fig. 6, a and c) (Huisman and d'Ari 1981). Consistent with their sensitivity to ciprofloxacin (Fig. 5), mutations in *rep*, *lexA*, or *polA* also resulted in increased MuGam-GFP focus formation (Fig. 6b and Supplementary Fig. 3, a, b, and d) and cell length (Fig. 6c and Supplementary Fig. 3c). Notably, a *rdgC* mutant displayed significant accumulation of DSBs (Supplementary Fig. 3, a, b, and d) while exhibiting only a moderate increase in cell length (Supplementary Fig. 3c) and no observable sensitization to ciprofloxacin (Supplementary Fig. 2).

The evidence of DSB accumulation and cell filamentation in other mutants tested is less compelling. Mutations in *priC*, *uup*, or *rdgB* produce only mild filamentation phenotypes, and there was limited evidence that disrupting *priC* enhances DSB levels (Supplementary Fig. 3, a–d). In fact, *nagC* and *rdgB* mutant strains exhibited significantly lower abundance of MuGam-GFP foci compared to the *wt* control and GFP focus levels in the *nagC* mutant approached the lower limit of detection. For the *nagC* mutant, this may have been caused by a significantly lower level of mean fluorescence (Supplementary Fig. 3e).
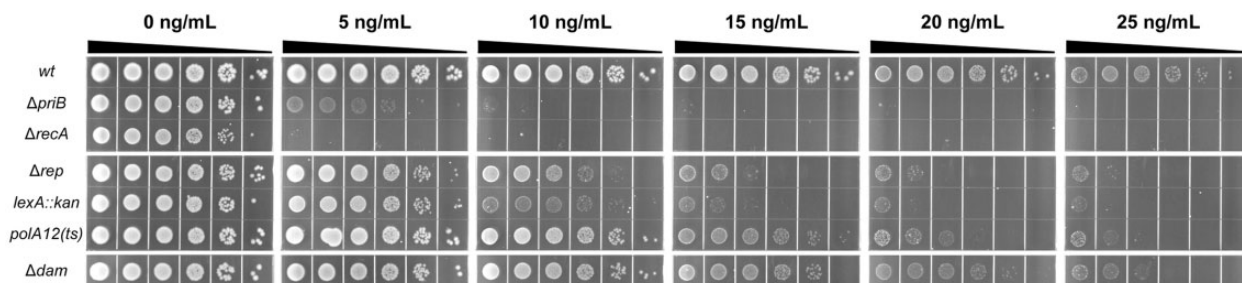
Fig. 5. Effects of *priB*, *rep*, *lexA*, *polA*, or *dam* mutations on DNA-damage sensitivity in *E. coli*. Sensitivity of mutants to DSBs was examined by spot plating on LB agar with 0–25 ng/ml ciprofloxacin. A *recA* deletion strain was utilized as a positive control of ciprofloxacin hypersensitivity. Dilutions (from left to right) are 10× serial dilutions from normalized overnight culture. Displayed spot plate data are representative of three replicates.
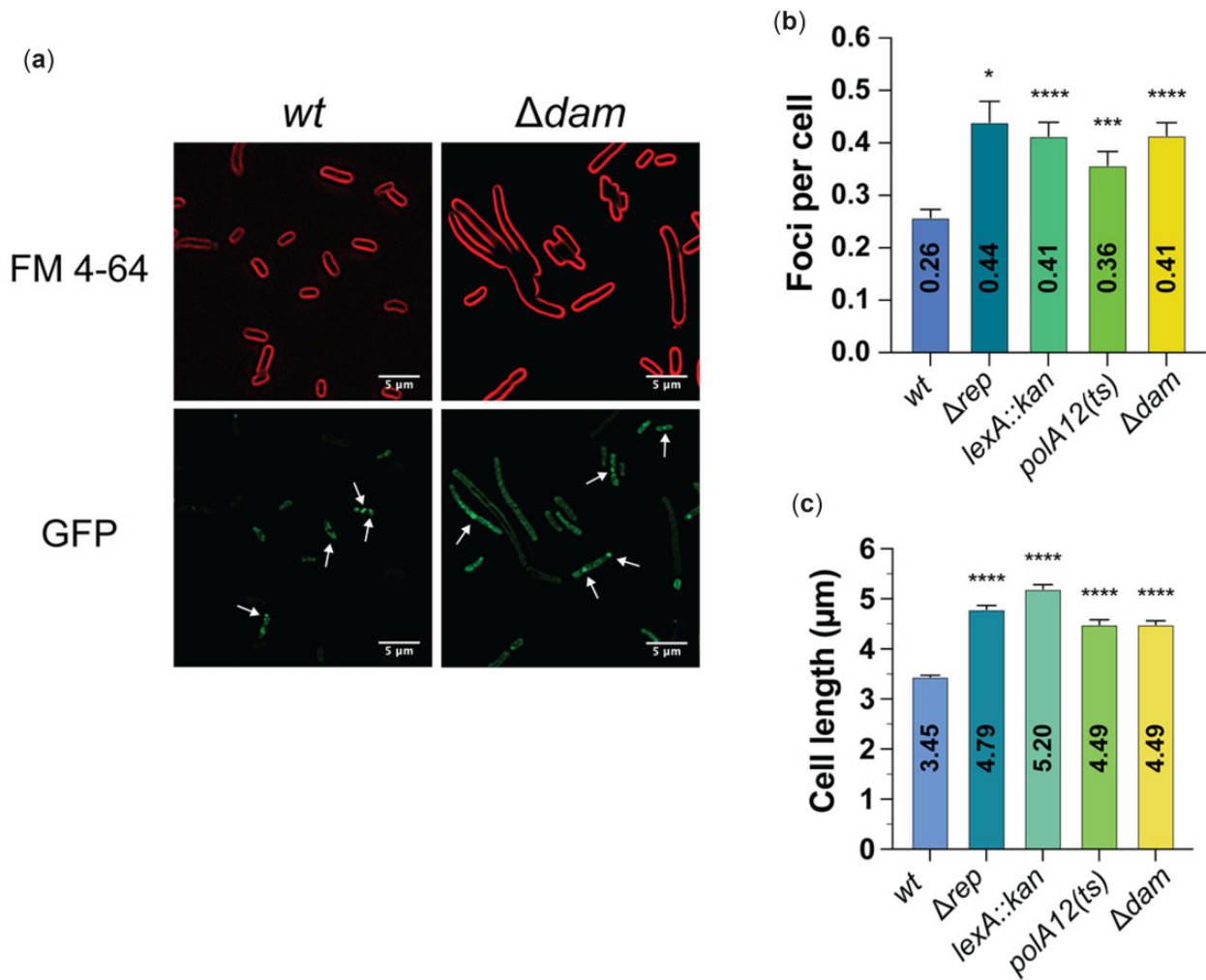
Fig. 6. Enhanced DSB formation in mutant *E. coli* strains. a) Representative images depicting MuGam-GFP foci and FM 4-64-stained membranes for *wt* (left) and Δ*dam* (right) strains. The abundance of MuGam-GFP foci per cell (b) and measured cell lengths (c) are displayed for *wt*, Δ*rep*, *lexA::kan*, *polA12(ts)*, and Δ*dam* strains. b, c) Mean values are depicted with error bars representing standard error of the mean. Statistical significance (*U* Mann–Whitney) for each strain compared to the *wt* control is displayed: $P < 0.05$ (*), $P < 0.001$ (***), and $P < 0.0001$ (****).
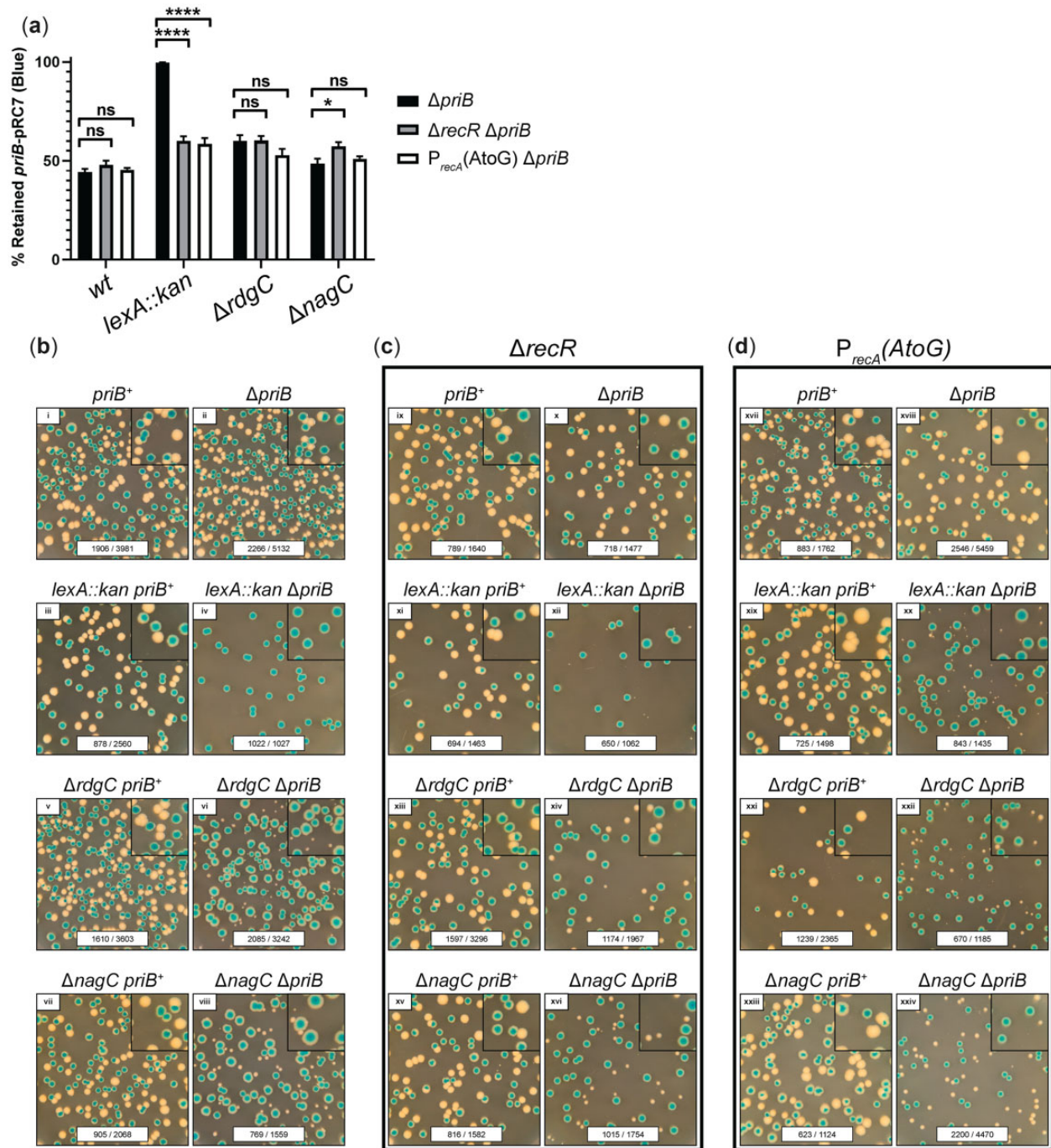
Modulating RecA function partially suppresses *lexA* or *rdgC* mutational effects on Δ*priB* cells

Mutations in *dam*, *rep*, *lexA*, *polA*, or *rdgC* increase DSB formation in vivo (Fig. 6, a and b and Supplementary Fig. 3, a, b, and d). In most cases, this effect is accompanied by sensitization to ciprofloxacin (Fig. 5 and Supplementary Fig. 2) and cell filamentation (Fig. 6c and Supplementary Fig. 3, a and c). Deleting *dam* or hindering Pol I polymerase activity can cause persistent ssDNA gaps that form DSBs when subsequent replisomes collide (Glickman 1975; Cao and Kogoma 1995; Mojas *et al.* 2007; Michel *et al.* 2018). Similarly, a loss of Rep accessory helicase activity correlates with more stalled replication forks that can create DSBs when they are encountered by subsequent replisomes (Michel *et al.* 1997; Seigneur *et al.* 1998; Michel *et al.* 2018). Our data strongly suggest an increase in DSB formation in *lexA* or *rdgC* mutants, which likely accounts for their genetic relationships with *priB*, but their mode of DSB formation is less clear.

Previous work has shown that loss of PriA or Rep helicase activity at stalled replication forks can cause inappropriate RecA recombinase loading mediated by the ssDNA gap repair proteins RecFOR (Mahdi *et al.* 2006). After it is loaded by RecFOR, RecA is hypothesized to reverse a stalled replication fork to form a

Holliday junction, also known as a "chicken-foot" structure (Robu *et al.* 2001; Courcelle *et al.* 2003). Because LexA or RdgC inhibit the activity of cellular RecA [via transcriptional repression (d'Ari 1985) or physical inhibition (Drees *et al.* 2006), respectively], we hypothesized that more stalled forks were reversed in *lexA* or *rdgC* mutants. The DSBs observed in vivo (Fig. 6b and Supplementary Fig. 3, a and b) could form in these mutants when the "chicken-foot" structures were encountered by additional replisomes (from multifork replication conditions in rich media) or upon processing by RuvABC, the Holliday junction resolvase (Seigneur *et al.* 1998, 2000; Withers and Bernander 1998; Michel *et al.* 2018).

To test this hypothesis, we examined the effect of RecA modulation on *lexA* or *rdgC* mutants in the *priB*-pRC7 plasmid retention assay (Fig. 7). Previously, our results identified a conditional essentiality of *lexA* in Δ*priB* cells based on robust retention of the *priB*-pRC7 plasmid (Figs. 3e and 7, a and b). After deleting *recR* in this strain (inactivating the RecFOR pathway), we observed viable *lexA::kan* Δ*priB* white colonies (Fig. 7c). The resulting colonies were quite small, consistent with growth defects, but these results strongly support a partial suppression of *lexA::kan* Δ*priB* via *recR* deletion. Likewise, the conditional importance of *rdgC* in Δ*priB* cells (Fig. 3g) was partially suppressed with a *recR* deletion,

Fig. 7. Modulating RecA activity partially suppresses mutational effects on Δ*priB E. coli.* a) Plasmid (*priB*-pRC7) retention in Δ*priB* strains is shown along with strains also carrying a *recR* deletion or *recA* promoter mutation. Mean values are depicted with error bars representing standard error of the mean. Statistical significance (unpaired Student's *t*-test) for each strain pair is displayed: $P < 0.05$ (*) and $P < 0.0001$ (****). b) Representative images of *priB*-pRC7 assay plates are presented for *wt*, *lexA::kan*, Δ*rdgC*, and Δ*nagC* strains with or without chromosomal *priB*. This experiment was extended to strains with (c) a *recR* deletion or (d) a mutation in *recA*'s promoter. b–d) Each image includes raw colony counts for each condition (# of blue colonies/# of total colonies). To better visualize small white colonies, 2.25× magnified insets are included in the upper right-hand corner. Each plate was incubated at 37°C for 22 h.

evidenced by significantly larger plasmid-less white colonies (Fig. 7c).

In addition to restricting the scope of RecA activity *in vivo* with a *recR* deletion, we hypothesized that reducing the cellular levels of RecA would also produce a suppressive effect. To accomplish this, we utilized a *recA* promoter mutation, P$_{recA}$(AtoG), which decreases *recA* expression (Weisemann and Weinstock 1985; 1991; Romero, Chen, *et al.* 2020). This mutation also suppressed

the effects of *lexA* or *rdgC* mutations in Δ*priB* cells, and the degree of suppression was strikingly similar to that of a *recR* deletion (Fig. 7d). To rule out general suppression ability of these RecA modulations, we tested their effect on other mutants identified in our *Tn*-seq screen. We only observed modest evidence of suppression by RecA modulation in Δ*nagC* Δ*priB* strains when comparing the relative sizes of white and blue colonies (Fig. 7, b–d). Taken together, these results suggest that *lexA* or *rdgC* deletions

promote inappropriate and/or excessive RecA activity causing stalled replication forks to physically reverse and eventually devolve to DSBs upon replisome collision or Holliday junction processing.

Discussion

DNA replication restart reactivates prematurely abandoned DNA replication sites that have failed due to replisome encounters with damaged DNA or proteins tightly bound to chromosomes. Our knowledge of the coordination between DNA replication restart and other genome maintenance pathways has been limited by a lack of systematic genetic studies assessing the importance of genes to each replication restart pathway in *E. coli*. To determine links between replication restart and other cellular processes, we have identified genes that are conditionally essential or important in *E. coli* strains with inactivated replication restart pathways. High-density transposon mutant libraries in strains lacking *priB*, *priC*, or with the *priA300* mutation were analyzed after growth on rich media. These mutations inactivate the PriA/PriB, PriC/Rep and PriA/PriC, or PriA/PriC pathways, respectively (Fig. 1) (Sandler 2000). Comparison of transposon-insertion profiles to a *wt* control strain revealed genetic interactions with specific replication restart pathways. It is possible these replication restart mutations elicit other cellular effects such as perturbations in gene expression levels, and these off-target impacts may affect cellular function. Future transcriptome experiments will help determine if the effects of these mutations are restricted to DNA replication restart pathway accessibility.

Several genes were found to be conditionally essential or important in Δ*priB E. coli*, which specifically lacks the PriA/PriB pathway (Fig. 2 and Supplementary Fig. 1a). In contrast, only one gene (*rep*) displayed significant importance in *priA300 E. coli* and no genes were significantly conditionally important in *priC::kan E. coli* (Supplementary Fig. 1, b and c). These results point to PriA/PriB serving as the major replication restart pathway integrated within the larger genome maintenance program in *E. coli*, consistent with prior data (Flores *et al.* 2002). It is possible that the PriA/PriC and PriC/Rep pathways operate on DNA replication fork substrates that are rarely generated under the conditions tested in our experiments (Heller and Marians 2005a). It is also possible that the PriA/PriB pathway can compensate for the PriA/PriC and PriC/Rep pathways but the latter two pathways cannot compensate for PriA/PriB.

Deletion of *rep* was found to be detrimental in both Δ*priB* and *priA300* strains, consistent with a general importance of the Rep helicase in genome maintenance (Fig. 2 and Supplementary Fig. 1c). Rep can be recruited to stalled replication forks via interaction with PriC where it helps facilitate DNA replication restart in the PriC/Rep pathway (Fig. 1) (Syeda *et al.* 2019; Nguyen *et al.* 2021). PriC interaction with Rep also stimulates its helicase activity (Heller and Marians 2005b). It may be that Δ*priB* and *priA300 E. coli* strains rely more heavily on the PriC/Rep pathway or that deletion of *rep* places a larger burden on the PriA/PriB or PriA/PriC DNA replication pathways. In accordance with the latter possibility, Rep also interacts with the replicative helicase, DnaB, which localizes Rep helicase activity to sites of DNA replication and is thought to enhance its ability to remove tightly associated protein barriers ahead of the replication fork (Syeda *et al.* 2019). The absence of Rep results in increased fork stalling, replisome dissociation, and DSBs if left unrepaired, which could also feed into the PriA/PriB pathway (Fig. 8) (Michel *et al.* 1997, 2018; Seigneur *et al.* 1998).

In addition to the known importance of *rep* in Δ*priB* cells, our results corroborated the importance of *dam* and *priC* in Δ*priB* cells (Fig. 3, c and f) (Sandler 2000; Boonsombat *et al.* 2006). In cells lacking Dam methyltransferase, both DNA strands are nicked and excised at equal frequency by methyl-directed mismatch repair enzymes, causing persistent ssDNA gaps that lead to DSBs when encountered by a replisome (Fig. 8) (Mojas *et al.* 2007; Michel *et al.* 2018). Interestingly, Δ*dam* cells are also associated with chromosomal overreplication, likely stemming from DSB repair feeding into DNA replication restart (Raghunathan *et al.* 2019). Overreplication could exacerbate DSB accumulation in Δ*dam* cells and it may elicit a similar effect in other DSB-causing mutants described in this study. The synthetic lethality of the Δ*priB* Δ*priC* combination was also confirmed (Fig. 3c), although the genetic relationship was not detected in either the Δ*priB* or *priC::kan* Tn-seq screens due to a small number of transpositions insertions mapped for *priB* or *priC* in the *wt* reference strain (Fig. 2 and Supplementary Fig. 1b). This may be due to a transposition recalcitrance for *priC* as has been noted for *priB* (Goodall *et al.* 2018). Thus, it is possible that additional *priB*, *priC*, or *priA300* genetic interactions beyond those described here may exist and that limitations of the Tn-seq approach could mask their identification.

The Tn-seq results in the Δ*priB* strain and targeted genetic experiments identified a host of novel *priB* genetic interactors: *lexA*, *polA*, *rdgC*, *uup*, *nagC*, and *rdgB* (Figs. 2 and 3). In addition to mutant strains expected to exhibit DSB accumulation (*rep* and *dam*), in vivo measurements detected significant DSB accumulation for *lexA*, *polA*, and *rdgC* mutants (Fig. 6, a and b and Supplementary Fig. 3, a and b). Formation of DSBs in these mutant strains was correlated with longer cell lengths (Fig. 6c and Supplementary Fig. 3c) and sensitization to the DSB-inducing antibiotic ciprofloxacin (Fig. 5 and Supplementary Fig. 2), except for the *rdgC* deletion.

Pol I is known to utilize its polymerase activity to fill ssDNA gaps during Okazaki fragment synthesis and following DNA repair (Lehman and Chien 1973; Glickman 1975; Uyemura and Lehman 1976; Cao and Kogoma 1995). The results shown here suggest this activity is especially important in Δ*priB* cells (Figs. 2b and 4b). We hypothesize that persistent ssDNA gaps are formed in *polA12(ts)* mutant strains at elevated temperatures, which lead to DSBs if left unrepaired when encountered by a replisome (Fig. 8) (Michel *et al.* 2018). This notion is supported by *polA12(ts)* Δ*priB* phenotype suppression on minimal media (Fig. 4b) when multifork DNA replication is less likely to occur and cause DSBs from collisions with ssDNA gaps (Withers and Bernander 1998; Fossum *et al.* 2007; Hill *et al.* 2012).

The formation of DSBs in *lexA* or *rdgC* deletion strains is less straightforward. Previous work has shown that the absence of PriA or Rep helicase activity can allow the RecFOR mediator proteins to inappropriately load RecA at stalled replication forks (Moore *et al.* 2003; Mahdi *et al.* 2006). Upon binding, RecA can physically reverse the stalled fork forming a "chicken-foot" structure (Fig. 8). DSBs will form from these structures when they are encountered by subsequent replication forks or when they are processed by RuvABC (Fig. 8) (Seigneur *et al.* 1998, 2000; Withers and Bernander 1998; Michel *et al.* 2018). Therefore, we hypothesized that the higher levels of DSBs formed in *lexA* or *rdgC* mutants (Fig. 6b and Supplementary Fig. 3, a, b, and d) was caused by excessive RecA activity: either by disrupting its transcriptional repressor (LexA) or by removing a RecA inhibitor (RdgC). Increasing the activity of RecA by disrupting *lexA* or *rdgC* would in turn promote unwarranted RecA activity (Fig. 8).
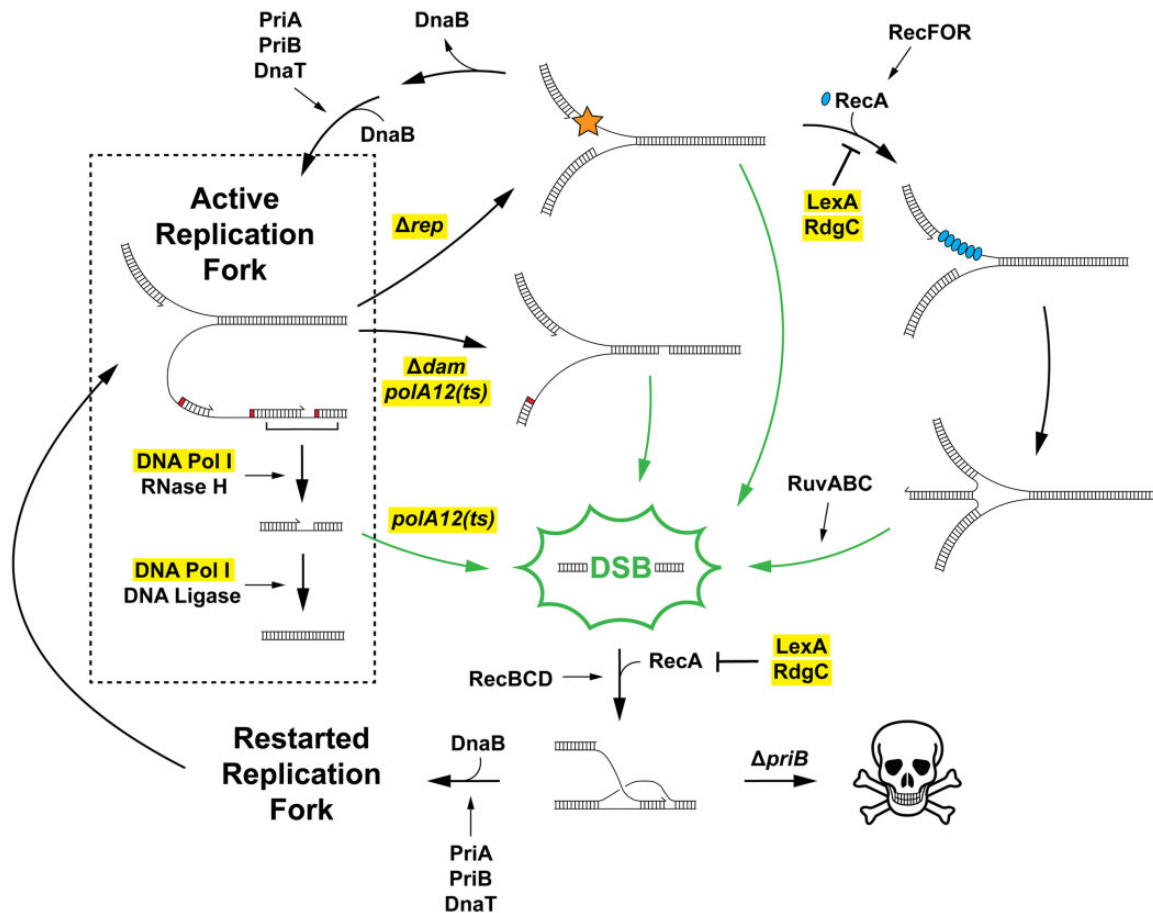
Fig. 8. DSBs accumulate from a variety of sources and are funneled into the PriA/PriB replication restart pathway following their repair. An active replication fork facilitates continuous DNA synthesis on the leading strand, while lagging strand synthesis is discontinuous and downstream processing is required by other enzymes. These productive processes are contained within the box. Several damaging paths are also shown. Loss of Rep causes an increase in replication fork collisions with nucleo-protein complexes (star). The most severe collisions cause lethal replisome dissociation unless DNA replication restart is carried out, which is primarily facilitated by the PriA/PriB pathway. Increased mismatch repair (without Dam methylation) or loss of Pol I polymerase activity following DNA repair or during Okazaki fragment maturation cause persistent ssDNA gaps. RecA loading at stalled replication forks mediated by RecFOR can drive fork reversal, which is inhibited by LexA or RdgC. Stalled/reversed replication forks and ssDNA gaps are DSB-prone substrates; if they are not efficiently repaired, they lead to DSBs when they are encountered by subsequent replisomes. When DSBs form, they are recognized and repaired with homologous recombination (RecA is loaded via RecBCD pathway). The resulting D-loop substrate is shuttled into the PriA/PriB pathway to reinitiate DNA replication and maintain cell viability. The genes/proteins examined with targeted genetic analyses in this study are highlighted.

Consistent with this notion, the effects of *lexA* or *rdgC* mutations on Δ*priB* cells were partially suppressed by disabling the RecFOR pathway (with a *recR* deletion) or by inhibiting cellular RecA activity by decreasing its expression with a promoter mutation (P*recA*(AtoG)) (Fig. 7). Future experiments are required to probe these relationships further by attempting suppression with deletion of *ruvC* (Fig. 8). Notably, the Δ*recR* and P*recA*(AtoG) suppression attempts partially restored the growth rates of Δ*rdgC* Δ*priB* colonies, while permitting (albeit limited) viability of *lexA::kan* Δ*priB* cells. It is likely that the SOS DNA-damage response induces the expression of one or more genes (other than *recA*) that are harmful to Δ*priB* cells.

DSBs can form in a variety of different ways in the cell. Disrupting genes identified in the Δ*priB* Tn-seq screen likely increased DSB levels by promoting the formation of DSB-prone substrates (stalled/reversed replication forks and ssDNA gaps), which are encountered by subsequent replication complexes in rich media (Fig. 8) (Withers and Bernander 1998; Fossum *et al.* 2007; Hill *et al.* 2012; Michel *et al.* 2018). While DSBs are

problematic, cells can survive if they are readily recognized and repaired. In *E. coli*, DSB repair is usually carried out by RecBCD, which processes DSBs before loading RecA to catalyze strand invasion and create a D-loop site for DNA replication restart (Fig. 8) (Dillingham and Kowalczykowski 2008). The DSBs formed in *rep*, *lexA*, *polA*, *dam*, and *rdgC* mutants can still be recognized and repaired by the RecBCD pathway to form D-loops, which subsequently undergo DNA replication restart via the PriA/PriB pathway (Heller and Marians 2005a; Boonsombat *et al.* 2006; Sasaki *et al.* 2007; Windgassen, Leroux, *et al.* 2018). We hypothesize that these mutations are synergistic with a *priB* deletion because DSBs are committed to a nonproductive pathway (when *priB* is absent) and stagnant D-loops may ultimately lead to cell death (Fig. 8). Furthermore, while most DSB-causing mutants showed some sensitization to ciprofloxacin, *priB* and *recA* deletion strains exhibited extreme sensitization, with *priB* deletion sensitizing cells just slightly less than a *recA* deletion (Fig. 5). Taken together, our data strengthen the experimental support for a link between DSB repair and the PriA/PriB pathway of DNA replication restart.

Our results do not exclude the possibility that the PriA/PriC or PriC/Rep pathways play more minor roles in replication restart after DSB repair as has been recently suggested (Mallikarjun and Gowrishankar 2022).

The results presented here highlight a variety of new questions and exciting opportunities of study. While *uup*, *nagC*, and *rdgB* are conditionally important in Δ*priB* cells, their disruption does not appear to cause DSBs in the conditions tested (Supplementary Fig. 3, a, b, and d). Most puzzling is the genetic relationship between *priB* and *nagC*, a transcriptional repressor that coordinates the biosynthesis of *N*-acetylglucosamine, a component of the bacterial cell wall (Plumbridge 2001; Pennetier *et al.* 2008). Deletion of *nagC* led to an aberrant cell morphology (Supplementary Fig. 3a), which may have caused the mutant's extremely low level of mean fluorescence in our experiments (Supplementary Fig. 3e). It is possible the perturbed cell membrane morphology is linked to DNA damage, similar to observations made with perturbed nuclear envelopes upon loss of lamin proteins in cancer cells (Denais *et al.* 2016). It is also possible that deletions of *uup*, *nagC*, or *rdgB* directly impact PriC-dependent replication restart, which would result in strong genetic interactions with *priB*. Future studies will be required to further probe these possibilities. Taken together, our findings have better defined a primary role for the PriA/PriB replication restart pathway following DSB repair in *E. coli* and have established important links that integrate replication restart processes into a larger genome maintenance program in bacteria.

Data availability

Raw sequencing data for *Tn*-seq experiments can be found at NCBI SRA under BioProject ID PRJNA837116. All microscopy data can be found at Dryad repository (https://doi.org/10.5061/dryad.547d7wmbx).

Supplemental material is available at G3 online.

Conflicts of interest

None declared.

Literature cited

Baba T, Ara T, Hasegawa M, Takai Y, Okumura Y, Baba M, Datsenko KA, Tomita M, Wanner BL, Mori H. Construction of *Escherichia coli* k-12 in-frame, single-gene knockout mutants: the keio collection. Mol Syst Biol. 2006;2:2006.0008.

Barquist L, Mayho M, Cummins C, Cain AK, Boinett CJ, Page AJ, Langridge GC, Quail MA, Keane JA, Parkhill J. The TraDIS toolkit: sequencing and analysis for dense transposon mutant libraries. Bioinformatics (Oxford, England). 2016;32(7):1109–1111.

Bernhardt TG, de Boer PA. Screening for synthetic lethal mutants in *Escherichia coli* and identification of Envc (YibP) as a periplasmic septal ring factor with murein hydrolase activity. Mol Microbiol. 2004;52(5):1255–1269.

Bhasin A, Goryshin IY, Reznikoff WS. Hairpin formation in Tn5 transposition. J Biol Chem. 1999;274(52):37021–37029.

Bi E, Lutkenhaus J. Analysis of ftsZ mutations that confer resistance to the cell division inhibitor SulA (SfiA). J Bacteriol. 1990;172(10):5602–5609.

Boonsombat R, Yeh SP, Milne A, Sandler SJ. A novel dnaC mutation that suppresses priB rep mutant phenotypes in *Escherichia coli* K-12. Mol Microbiol. 2006;60(4):973–983.

Bradshaw JS, Kuzminov A. RdgB acts to avoid chromosome fragmentation in *Escherichia coli*. Mol Microbiol. 2003;48(6):1711–1725.

Burger BT, Imam S, Scarborough MJ, Noguera DR, Donohue TJ. Combining genome-scale experimental and computational methods to identify essential genes in *Rhodobacter sphaeroides*. mSystems. 2017;2(3):e00015–17.

Byrne RT, Chen SH, Wood EA, Cabot EL, Cox MM. *Escherichia coli* genes and pathways involved in surviving extreme exposure to ionizing radiation. J Bacteriol. 2014;196(20):3534–3545.

Camps M, Loeb LA. Critical role of R-loops in processing replication blocks. Front Biosci. 2005;10:689–698.

Cao Y, Kogoma T. The mechanism of recA polA lethality: suppression by RecA-independent recombination repair activated by the lexA(Def) mutation in *Escherichia* coli. Genetics. 1995;139(4):1483–1494.

Cherepanov PP, Wackernagel W. Gene disruption in *Escherichia coli*: TcR and KmR cassettes with the option of Flp-catalyzed excision of the antibiotic-resistance determinant. Gene. 1995;158(1):9–14.

Costa A, Hood IV, Berger JM. Mechanisms for initiating cellular DNA replication. Annu Rev Biochem. 2013;82:25–54.

Courcelle J, Donaldson JR, Chow K-H, Courcelle CT. DNA damage-induced replication fork regression and processing in *Escherichia coli*. Science (New York, NY). 2003;299(5609):1064–1067.

Cox MM, Goodman MF, Kreuzer KN, Sherratt DJ, Sandler SJ, Marians KJ. The importance of repairing stalled replication forks. Nature. 2000;404(6773):37–41.

d'Ari R. The SOS system. Biochimie. 1985;67(3–4):343–347.

Datsenko KA, Wanner BL. One-step inactivation of chromosomal genes in *Escherichia coli* K-12 using PCR products. Proc Natl Acad Sci U S A. 2000;97(12):6640–6645.

Denais CM, Gilbert RM, Isermann P, McGregor AL, Te Lindert M, Weigelin B, Davidson PM, Friedl P, Wolf K, Lammerding J. Nuclear

envelope rupture and repair during cancer cell migration. Science (New York, NY). 2016;352(6283):353–358.

Dillingham MS, Kowalczykowski SC. RecBCD enzyme and the repair of double-stranded DNA breaks. Microbiol Mol Biol Rev. 2008; 72(4):642–671.

Drees JC, Chitteni-Pattu S, McCaslin DR, Inman RB, Cox MM. Inhibition of RecA protein function by the RdgC protein from *Escherichia coli*. J Biol Chem. 2006;281(8):4708–4717.

Ducret A, Quardokus EM, Brun YV. MicrobeJ, a tool for high throughput bacterial cell detection and quantitative analysis. Nat Microbiol. 2016;1(7):16077.

Flores MJ, Ehrlich SD, Michel B. Primosome assembly requirement for replication restart in the *Escherichia coli* holDG10 replication mutant. Mol Microbiol. 2002;44(3):783–792.

Fossum S, Crooke E, Skarstad K. Organization of sister origins and replisomes during multifork DNA replication in *Escherichia coli*. EMBO J. 2007;26(21):4514–4522.

Giese KC, Michalowski CB, Little JW. RecA-dependent cleavage of LexA dimers. J Mol Biol. 2008;377(1):148–161.

Glickman BW. The role of DNA polymerase I in excision-repair. Basic Life Sci. 1975;5a:213–218.

Goodall ECA, Robinson A, Johnston IG, Jabbari S, Turner KA, Cunningham AF, Lund PA, Cole JA, Henderson IR. The essential genome of Escherichia coli K-12. mBio. 2018;9(1):e02096–17.

Goryshin IY, Reznikoff WS. Tn5 in vitro transposition. J Biol Chem. 1998;273(13):7367–7374.

Heller RC, Marians KJ. The disposition of nascent strands at stalled replication forks dictates the pathway of replisome loading during restart. Mol Cell. 2005a;17(5):733–743.

Heller RC, Marians KJ. Unwinding of the nascent lagging strand by Rep and PriA enables the direct restart of stalled replication forks. J Biol Chem. 2005b;280(40):34143–34151.

Henrikus SS, Henry C, Ghodke H, Wood EA, Mbele N, Saxena R, Basu U, van Oijen AM, Cox MM, Robinson A. RecFOR epistasis group: RecF and RecO have distinct localizations and functions in *Escherichia coli*. Nucleic Acids Res. 2019;47(6):2946–2965.

Hill NS, Kadoya R, Chattoraj DK, Levin PA. Cell size and the initiation of DNA replication in bacteria. PLoS Genet. 2012;8(3):e1002549.

Huang LC, Wood EA, Cox MM. Convenient and reversible site-specific targeting of exogenous DNA into a bacterial chromosome by use of the FLP recombinase: the FLIRT system. J Bacteriol. 1997;179(19):6076–6083.

Huisman O, d'Ari R. An inducible DNA replication-cell division coupling mechanism in *E. coli*. Nature. 1981;290(5809):797–799.

Joyce CM, Fujii DM, Laks HS, Hughes CM, Grindley ND. Genetic mapping and DNA sequence analysis of mutations in the polA gene of *Escherichia coli*. J Mol Biol. 1985;186(2):283–293.

Joyce CM, Grindley ND. Method for determining whether a gene of *Escherichia coli* is essential: application to the polA gene. J Bacteriol. 1984;158(2):636–643.

Kim S, Dallmann HG, McHenry CS, Marians KJ. Coupling of a replicative polymerase and helicase: a tau-DnaB interaction mediates rapid replication fork movement. Cell. 1996a;84(4):643–650.

Kim S, Dallmann HG, McHenry CS, Marians KJ. Tau protects beta in the leading-strand polymerase complex at the replication fork. J Biol Chem. 1996b;271(8):4315–4318.

Kim T, Chitteni-Pattu S, Cox BL, Wood EA, Sandler SJ, Cox MM. Directed evolution of RecA variants with enhanced capacity for conjugational recombination. PLoS Genet. 2015;11(6):e1005278.

Klenow H, Henningsen I. Selective elimination of the exonuclease activity of the deoxyribonucleic acid polymerase from *Escherichia coli* B by limited proteolysis. Proc Natl Acad Sci U S A. 1970;65(1): 168–175.

Klitgaard RN, Jana B, Guardabassi L, Nielsen KL, Løbner-Olesen A. DNA damage repair and drug efflux as potential targets for reversing low or intermediate ciprofloxacin resistance in *E. coli* K-12. Front Microbiol. 2018;9:1438.

Kogoma T. Stable DNA replication: interplay between DNA replication, homologous recombination, and transcription. Microbiol Mol Biol Rev. 1997;61(2):212–238.

Langmead B, Salzberg SL. Fast gapped-read alignment with Bowtie 2. Nat Methods. 2012;9(4):357–359.

Langridge GC, Phan M-D, Turner DJ, Perkins TT, Parts L, Haase J, Charles I, Maskell DJ, Peters SE, Dougan G, *et al.* Simultaneous assay of every *Salmonella typhi* gene using one million transposon mutants. Genome Res. 2009;19(12):2308–2316.

Lee EH, Kornberg A. Replication deficiencies in priA mutants of *Escherichia coli* lacking the primosomal replication n' protein. Proc Natl Acad Sci U S A. 1991;88(8):3029–3032.

Lehman IR, Chien JR. Persistence of deoxyribonucleic acid polymerase i and its 5'–3' exonuclease activity in PolA mutants of *Escherichia coli* K12. J Biol Chem. 1973;248(22):7717–7723.

Mahdi AA, Buckman C, Harris L, Lloyd RG. Rep and PriA helicase activities prevent RecA from provoking unnecessary recombination during replication fork repair. Genes Dev. 2006;20(15):2135–2147.

Mallikarjun J, Gowrishankar J. Essential role for an isoform of *Escherichia coli* translation initiation factor IF2 in repair of two-ended DNA double-strand breaks. J Bacteriol. 2022;204(4):e0057121.

Mangiameli SM, Merrikh CN, Wiggins PA, Merrikh H. Transcription leads to pervasive replisome instability in bacteria. eLife. 2017;6: e19848.

Manhart CM, McHenry CS. The PriA replication restart protein blocks replicase access prior to helicase assembly and directs template specificity through its ATPase activity. J Biol Chem. 2013;288(6): 3989–3999.

Marinus MG. Recombination is essential for viability of an *Escherichia coli* dam (DNA adenine methyltransferase) mutant. J Bacteriol. 2000;182(2):463–468.

Martin M. Cutadapt removes adapter sequences from high-throughput sequencing reads. EMBnetjournal. 2011;17(1):3.

Masai H, Asai T, Kubota Y, Arai K, Kogoma T. *Escherichia coli* PriA protein is essential for inducible and constitutive stable DNA replication. EMBO J. 1994;13(22):5338–5345.

McCool JD, Ford CC, Sandler SJ. A dnaT mutant with phenotypes similar to those of a priA2::Kan mutant in *Escherichia coli* K-12. Genetics. 2004;167(2):569–578.

McCool JD, Long E, Petrosino JF, Sandler HA, Rosenberg SM, Sandler SJ. Measurement of SOS expression in individual *Escherichia coli* K-12 cells using fluorescence microscopy. Mol Microbiol. 2004;53(5): 1343–1357.

Michel B, Ehrlich SD, Uzest M. DNA double-strand breaks caused by replication arrest. EMBO J. 1997;16(2):430–438.

Michel B, Sandler SJ. Replication restart in bacteria. J Bacteriol. 2017; 199(13):e00102–17.

Michel B, Sinha AK, Leach DRF. Replication fork breakage and restart in *Escherichia coli*. Microbiol Mol Biol Rev. 2018;82(3):e00013–18.

Mojas N, Lopes M, Jiricny J. Mismatch repair-dependent processing of methylation damage gives rise to persistent single-stranded gaps in newly replicated DNA. Genes Dev. 2007;21(24):3342–3355.

Moore T, McGlynn P, Ngo HP, Sharples GJ, Lloyd RG. The RdgC protein of *Escherichia coli* binds DNA and counters a toxic effect of RecFOR in strains lacking the replication restart protein PriA. EMBO J. 2003;22(3):735–745.

Murat D, Bance P, Callebaut I, Dassa E. ATP hydrolysis is essential for the function of the Uup ATP-binding cassette ATPase in precise excision of transposons. J Biol Chem. 2006;281(10):6850–6859.

Nguyen B, Shinn MK, Weiland E, Lohman TM. Regulation of *E. coli* rep helicase activity by PriC. J Mol Biol. 2021;433(15):167072.

Nowosielska A, Marinus MG. Cisplatin induces DNA double-strand break formation in *Escherichia coli* dam mutants. DNA Repair (Amst). 2005;4(7):773–781.

Nurse P, Zavitz KH, Marians KJ. Inactivation of the *Escherichia coli* priA DNA replication protein induces the SOS response. J Bacteriol. 1991;173(21):6686–6693.

Pennetier C, Domínguez-Ramírez L, Plumbridge J. Different regions of Mlc and NagC, homologous transcriptional repressors controlling expression of the glucose and N-acetylglucosamine phosphotransferase systems in *Escherichia coli*, are required for inducer signal recognition. Mol Microbiol. 2008;67(2):364–377.

Plumbridge J. DNA binding sites for the Mlc and NagC proteins: regulation of nagE, encoding the N-acetylglucosamine-specific transporter in *Escherichia coli*. Nucleic Acids Res. 2001;29(2):506–514.

Raghunathan N, Goswami S, Leela JK, Pandiyan A, Gowrishankar J. A new role for *Escherichia coli* Dam DNA methylase in prevention of aberrant chromosomal replication. Nucleic Acids Res. 2019; 47(11):5698–5711.

Robu ME, Inman RB, Cox MM. RecA protein promotes the regression of stalled replication forks in vitro. Proc Natl Acad Sci U S A. 2001; 98(15):8211–8218.

Romero ZJ, Armstrong TJ, Henrikus SS, Chen SH, Glass DJ, Ferrazzoli AE, Wood EA, Chitteni-Pattu S, van Oijen AM, Lovett ST, *et al.* Frequent template switching in postreplication gaps: suppression of deleterious consequences by the *Escherichia coli* Uup and RadD proteins. Nucleic Acids Res. 2020;48(1):212–230.

Romero ZJ, Chen SH, Armstrong T, Wood EA, van Oijen A, Robinson A, Cox MM. Resolving toxic DNA repair intermediates in every *E. coli* replication cycle: critical roles for RecG, Uup and RadD. Nucleic Acids Res. 2020;48(15):8445–8460.

Sandler SJ. Multiple genetic pathways for restarting DNA replication forks in *Escherichia coli* K-12. Genetics. 2000;155(2):487–497.

Sandler SJ, Leroux M, Windgassen TA, Keck JL. *Escherichia coli* K-12 has two distinguishable PriA-PriB replication restart pathways. Mol Microbiol. 2021;116(4):1140–1150.

Sandler SJ, Marians KJ, Zavitz KH, Coutu J, Parent MA, Clark AJ. dnaC mutations suppress defects in DNA replication- and recombination-associated functions in priB and priC double mutants in *Escherichia coli* K-12. Mol Microbiol. 1999;34(1):91–101.

Sandler SJ, McCool JD, Do TT, Johansen RU. PriA mutations that affect PriA-PriC function during replication restart. Mol Microbiol. 2001;41(3):697–704.

Sasaki K, Ose T, Okamoto N, Maenaka K, Tanaka T, Masai H, Saito M, Shirai T, Kohda D. Structural basis of the 3'-end recognition of a leading strand in stalled replication forks by PriA. EMBO J. 2007; 26(10):2584–2593.

Savic DJ, Jankovic M, Kostic T. Cellular role of DNA polymerase I. J Basic Microbiol. 1990;30(10):769–784.

Seigneur M, Bidnenko V, Ehrlich SD, Michel B. RuvAB acts at arrested replication forks. Cell. 1998;95(3):419–430.

Seigneur M, Ehrlich SD, Michel B. RuvABC-dependent double-strand breaks in dnaBts mutants require recA. Mol Microbiol. 2000;38(3): 565–574.

Shee C, Cox BD, Gu F, Luengas EM, Joshi MC, Chiu LY, Magnan D, Halliday JA, Frisch RL, Gibson JL, *et al.* Engineered proteins detect spontaneous DNA breakage in human and bacterial cells. eLife. 2013;2:e01222.

Singer M, Baker TA, Schnitzler G, Deischel SM, Goel M, Dove W, Jaacks KJ, Grossman AD, Erickson JW, Gross CA. A collection of strains containing genetically linked alternating antibiotic resistance elements for genetic mapping of *Escherichia coli*. Microbiol Rev. 1989;53(1):1–24.

Sutera VA, Jr, Lovett ST. The role of replication initiation control in promoting survival of replication fork damage. Mol Microbiol. 2006;60(1):229–239.

Syeda AH, Wollman AJM, Hargreaves AL, Howard JAL, Brüning JG, McGlynn P, Leake MC. Single-molecule live cell imaging of rep reveals the dynamic interplay between an accessory replicative helicase and the replisome. Nucleic Acids Res. 2019;47(12): 6287–6298.

Tamayo M, Santiso R, Gosalvez J, Bou G, Fernández JL. Rapid assessment of the effect of ciprofloxacin on chromosomal DNA from *Escherichia coli* using an in situ DNA fragmentation assay. BMC Microbiol. 2009;9:69.

Tougu K, Peng H, Marians KJ. Identification of a domain of *Escherichia coli* primase required for functional interaction with the DnaB helicase at the replication fork. J Biol Chem. 1994;269(6): 4675–4682.

Uyemura D, Lehman IR. Biochemical characterization of mutant forms of DNA polymerase I from *Escherichia coli*. I. The polA12 mutation. J Biol Chem. 1976;251(13):4078–4084.

van Opijnen T, Bodi KL, Camilli A. Tn-seq: high-throughput parallel sequencing for fitness and genetic interaction studies in microorganisms. Nat Methods. 2009;6(10):767–772.

van Opijnen T, Camilli A. Transposon insertion sequencing: a new tool for systems-level analysis of microorganisms. Nat Rev Microbiol. 2013;11(7):435–442.

Weisemann JM, Weinstock GM. Direct selection of mutations reducing transcription or translation of the recA gene of *Escherichia coli* with a recA-lacZ protein fusion. J Bacteriol. 1985;163(2):748–755.

Weisemann JM, Weinstock GM. The promoter of the recA gene of *Escherichia coli*. Biochimie. 1991;73(4):457–470.

Willmott CJ, Maxwell A. A single point mutation in the DNA gyrase a protein greatly reduces binding of fluoroquinolones to the gyrase-DNA complex. Antimicrob Agents Chemother. 1993;37(1): 126–127.

Windgassen TA, Leroux M, Satyshur KA, Sandler SJ, Keck JL. Structure-specific DNA replication-fork recognition directs helicase and replication restart activities of the pria helicase. Proc Natl Acad Sci U S A. 2018;115(39):E9075–E9084.

Windgassen TA, Wessel SR, Bhattacharyya B, Keck JL. Mechanisms of bacterial DNA replication restart. Nucleic Acids Res. 2018; 46(2):504–519.

Withers HL, Bernander R. Characterization of dnaC2 and dnaC28 mutants by flow cytometry. J Bacteriol. 1998;180(7):1624–1631.

Communicating editor: N. Rhind